LETTERS
https://doi.org/10.1038/s41591-019-0746-2
nature medicine

Potent Zika and dengue cross-neutralizing antibodies induced by Zika vaccination in a dengue-experienced donor

Vincent Dussupt[1,2,3,17], Rajeshwer S. Sankhala[1,2,3,17], Gregory D. Gromowski[4,17], Gina Donofrio[1,2,3,17], Rafael A. De La Barrera[5], Rafael A. Larocca[6,7], Weam Zaky[1,2,3], Letzibeth Mendez-Rivera[1,2,3], Misook Choe[1,2,3], Edgar Davidson[8], Michael K. McCracken[4], James D. Brien[9], Peter Abbink[6,7], Hongjun Bai[1,2,3], Aubrey L. Bryan[8], Candace Hope Bias[5], Irina Maljkovic Berry[4], Nubia Botero[5], Tanya Cook[5], Nicole A. Doria-Rose[10], Ariadna Grinyo i Escuer[8], Justice Akuoku Frimpong[11], Aviva Geretz[1,2,3], Mayda Hernandez[8], Bradley S. Hollidge[11], Ningbo Jian[1,2,3], Kareem Kabra[5], David J. Leggat[10], Jinyan Liu[6,7], Amelia K. Pinto[9], Wiriya Rutvisuttinunt[4], Ian Setliff[12], Ursula Tran[1,2,3], Samantha Townsley[1,2,3], Benjamin J. Doranz[8], Morgane Rolland[1,2,3], Adrian B. McDermott[10], Ivelin S. Georgiev[12], Rasmi Thomas[1,2,3], Merlin L. Robb[2,3], Kenneth H. Eckels[5], Elizabeth Barranco[13], Michael Koren[4], Darci R. Smith[11,16], Richard G. Jarman[4], Sarah L. George[14], Kathryn E. Stephenson[6,7], Dan H. Barouch[6,7], Kayvon Modjarrad[1], Nelson L. Michael[15], M. Gordon Joyce[1,2,3*] and Shelly J. Krebs[1,2,3*]

Zika virus (ZIKV) has caused significant disease, with widespread cases of neurological pathology and congenital neurologic defects. Rapid vaccine development has led to a number of candidates capable of eliciting potent ZIKV-neutralizing antibodies (reviewed in refs. [1-3]). Despite advances in vaccine development, it remains unclear how ZIKV vaccination affects immune responses in humans with prior flavivirus immunity. Here we show that a single-dose immunization of ZIKV purified inactivated vaccine (ZPIV)[4-7] in a dengue virus (DENV)-experienced human elicited potent cross-neutralizing antibodies to both ZIKV and DENV. Using a unique ZIKV virion-based sorting strategy, we isolated and characterized multiple antibodies, including one termed MZ4, which targets a novel site of vulnerability centered on the Envelope (E) domain I/III linker region and protects mice from viremia and viral dissemination following ZIKV or DENV-2 challenge. These data demonstrate that Zika vaccination in a DENV-experienced individual can boost pre-existing flavivirus immunity and elicit protective responses against both ZIKV and DENV. ZPIV vaccination in Puerto Rican individuals with prior flavivirus experience yielded similar cross-neutralizing potency after a single vaccination, highlighting the potential benefit of ZIKV vaccination in flavivirus-endemic areas.

The induction of high titer neutralizing antibodies is a major goal of vaccination. We recently reported that two vaccinations of Zika virus (ZIKV) purified inactivated vaccine (ZPIV) in humans elicited potent neutralizing antibody responses (NCT02937233, NCT02963909)[7]. Passively transferred IgG from these participants was capable of protecting mice from ZIKV viremia[7]. Participant A from this trial showed remarkably high ZIKV neutralization titers, initially observed at two weeks following the first vaccination and at increased levels following the second vaccination (Fig. 1a). Serologic assays at baseline (week 0) found that this individual had previous flavivirus exposure, as high neutralizing antibody titers to dengue virus seroptypes 1–4 (DENV1–4) and West Nile virus (WNV) were detected prior to ZPIV vaccination (Fig. 1b). Following the

[1]Emerging Infectious Diseases Branch, Center of Infectious Disease Research, Walter Reed Army Institute of Research, Silver Spring, MD, USA. [2]U.S. Military HIV Research Program, Center of Infectious Disease Research, Walter Reed Army Institute of Research, Silver Spring, MD, USA. [3]Henry M. Jackson Foundation for the Advancement of Military Medicine, Bethesda, MD, USA. [4]Viral Diseases Branch, Center of Infectious Disease Research, Walter Reed Army Institute of Research, Silver Spring, MD, USA. [5]Pilot Bioproduction Facility, Center for Enabling Capabilities, Walter Reed Army Institute of Research, Silver Spring, MD, USA. [6]Center for Virology and Vaccine Research, Beth Israel Deaconess Medical Center, Harvard Medical School, Boston, MA, USA. [7]Ragon Institute of MGH, Cambridge, MA, USA. [8]Integral Molecular, Philadelphia, PA, USA. [9]Department of Molecular Microbiology and Immunology, Saint Louis University School of Medicine, Saint Louis, MO, USA. [10]Vaccine Research Center, NIAID, NIH, Bethesda, MD, USA. [11]U.S. Army Medical Research Institute of Infectious Diseases, Fort Detrick, MD, USA. [12]Vanderbilt Vaccine Center, Vanderbilt University Medical Center, Nashville, TN, USA. [13]Ponce Health Sciences University, CAIMED Center, Ponce, Puerto Rico, USA. [14]Department of Internal Medicine, Division of Infectious Diseases, Allergy and Immunology, Saint Louis University School of Medicine and St Louis VA Medical Center, Saint Louis, MO, USA. [15]Center of Infectious Disease Research, Walter Reed Army Institute of Research, Silver Spring, MD, USA. [16]Present address: Immunodiagnostics Department, Biological Defense Research Directorate, Naval Medical Research Center, Fort Detrick, MD, USA. [17]These authors contributed equally: Vincent Dussupt, Rajeshwer S. Sankhala, Gregory D. Gromowski, Gina Donofrio. *e-mail: gjoyce@eidresearch.org; skrebs@hivresearch.org

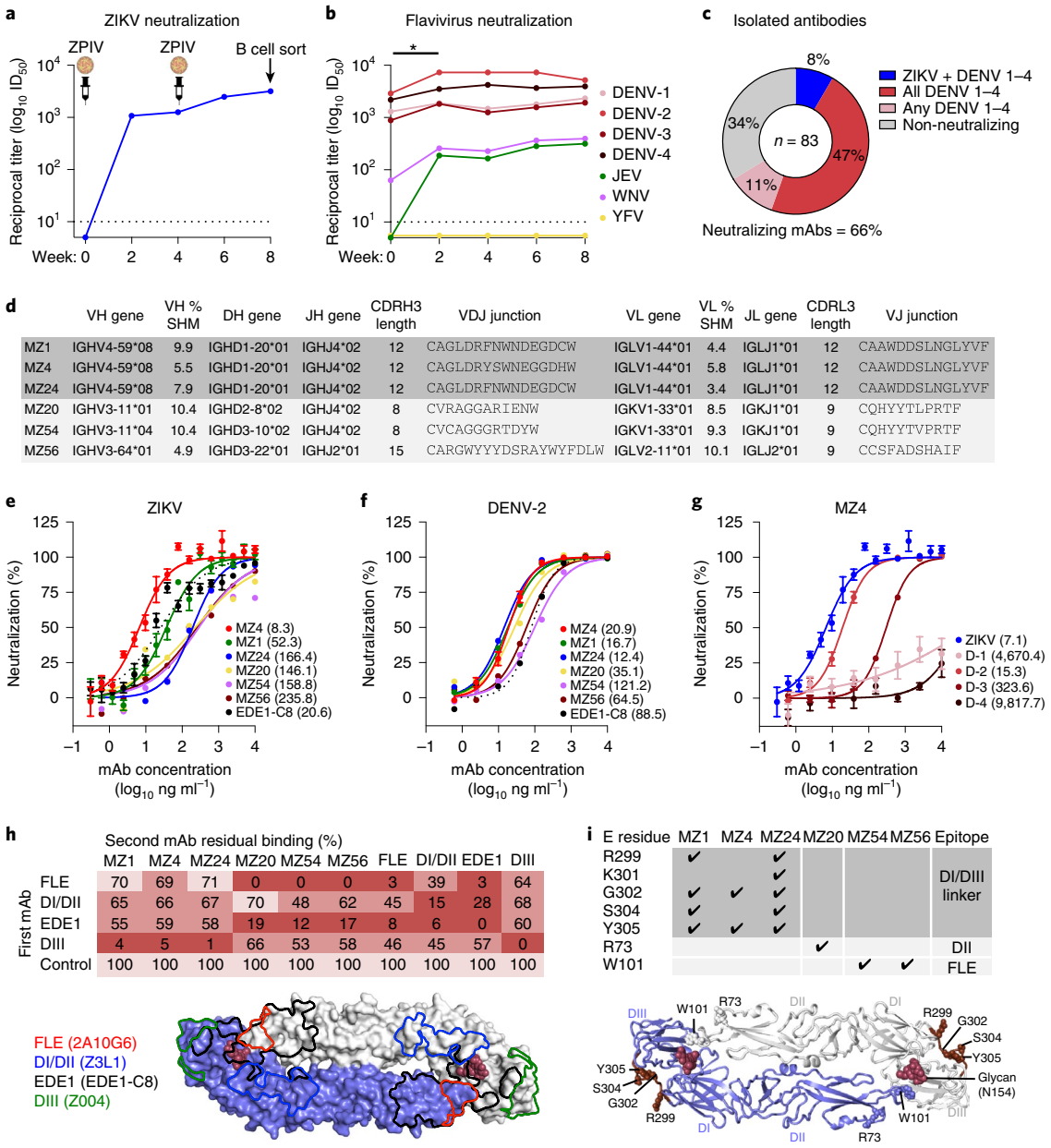

	VH gene	VH % SHM	DH gene	JH gene	CDRH3 length	VDJ junction	VL gene	VL % SHM	JL gene	CDRL3 length	VJ junction
MZ1	IGHV4-59*08	9.9	IGHD1-20*01	IGHJ4*02	12	CAGLDRFNWNDEGDCW	IGLV1-44*01	4.4	IGLJ1*01	12	CAAWDDSLNGLYVF
MZ4	IGHV4-59*08	5.5	IGHD1-20*01	IGHJ4*02	12	CAGLDRYSWNEGGDHW	IGLV1-44*01	5.8	IGLJ1*01	12	CAAWDDSLNGLYVF
MZ24	IGHV4-59*08	7.9	IGHD1-20*01	IGHJ4*02	12	CAGLDRFNWNDEGDCW	IGLV1-44*01	3.4	IGLJ1*01	12	CAAWDDSLNGLYVF
MZ20	IGHV3-11*01	10.4	IGHD2-8*02	IGHJ4*02	8	CVRAGGARIENW	IGKV1-33*01	8.5	IGKJ1*01	9	CQHYYTLPRTF
MZ54	IGHV3-11*04	10.4	IGHD3-10*02	IGHJ4*02	8	CVCAGGGRTDYW	IGKV1-33*01	9.3	IGKJ1*01	9	CQHYYTVPRTF
MZ56	IGHV3-64*01	4.9	IGHD3-22*01	IGHJ2*01	15	CARGWYYYDSRAYWYFDLW	IGLV2-11*01	10.1	IGLJ2*01	9	CCSFADSHAIF

First mAb \ Second mAb residual binding (%)	MZ1	MZ4	MZ24	MZ20	MZ54	MZ56	FLE	DI/DII	EDE1	DIII
FLE	70	69	71	0	0	0	3	39	3	64
DI/DII	65	66	67	70	48	62	45	15	28	68
EDE1	55	59	58	19	12	17	8	6	0	60
DIII	4	5	1	66	53	58	46	45	57	0
Control	100	100	100	100	100	100	100	100	100	100

E residue	MZ1	MZ4	MZ24	MZ20	MZ54	MZ56	Epitope
R299	✔		✔				DI/DIII linker
K301			✔				
G302	✔	✔	✔				
S304	✔		✔				
Y305	✔	✔	✔				
R73				✔			DII
W101					✔	✔	FLE

Fig. 1 | ZPIV vaccination boosts pre-existing immunity and elicits cross-neutralizing antibodies in a flavivirus-experienced individual. a,**b**, Vaccination schedule and plasma neutralizing antibody titers against ZIKV (**a**) and other flaviviruses (**b**) following ZPIV vaccination in participant A. A significant increase in flavivirus neutralization was found following the first vaccination, between week 0 and week 2 (two-tailed Wilcoxon matched-pairs signed-rank test, $P=0.036$, $n=7$ flaviviruses). Dotted lines indicate the limit of quantification of the assay. **c**, Summary of isolated mAbs at week 8. Eighty-three mAbs out of 116 bound to whole ZIKV and/or DENV-2 virions, with 66% of those mAbs neutralizing ZIKV and/or DENV1–4. **d**, Gene assignment and characteristics of the ZIKV-neutralizing mAbs with an inhibitory concentration at 50% (IC_{50}) <1 μg ml^{-1}. MZ4 family members are shaded in dark gray. SHM, somatic hypermutation; VDJ, variable, diversity and joining genes. **e**,**f**, Neutralization (FlowNT) against ZIKV (Paraiba_01) (**e**) and DENV-2 (S16803) (**f**). Error bars indicate mean ± s.e.m. from three independent experiments. For each mAb, the geometric mean inhibitory concentration (ng ml^{-1}) at 50% (IC_{50}) is indicated in parenthesis. **g**, MZ4 neutralization of ZIKV and DENV1–4. For each mAb, the geometric mean IC_{50} is indicated in parentheses. Error bars indicate mean ± s.e.m. from three independent experiments. **h**, Mapping of the ZIKV-neutralizing mAbs by binding competition. Top: identification of domain specificities. Values represent the % residual binding of the indicated second antibody after saturation of ZIKV E with the indicated first antibody. Shading from dark to light indicates competition strength ranging from strong (0–30%), to intermediate (31–69%), to weak/none (70–100%). Bottom: control antibody epitopes mapped onto the ZIKV E dimer structure. **i**, Shotgun mutagenesis prM/E epitope mapping. Top: residues critical for binding to ZIKV E (check marks) are indicated for each mAb. Bottom: indicated residues mapped on the E dimer.

first ZPIV vaccination, neutralization titers significantly increased ($P=0.036$) against several flaviviruses, including DENV1–4, WNV and Japanese encephalitis virus (JEV), but not yellow fever virus (YFV) (Fig. 1b). Following the second vaccination at week 4, neutralization titers increased against WNV and JEV, and were maintained against DENV1–4 (Fig. 1b).

To characterize the neutralizing antibodies elicited by ZPIV vaccination within this participant, we performed a unique B cell

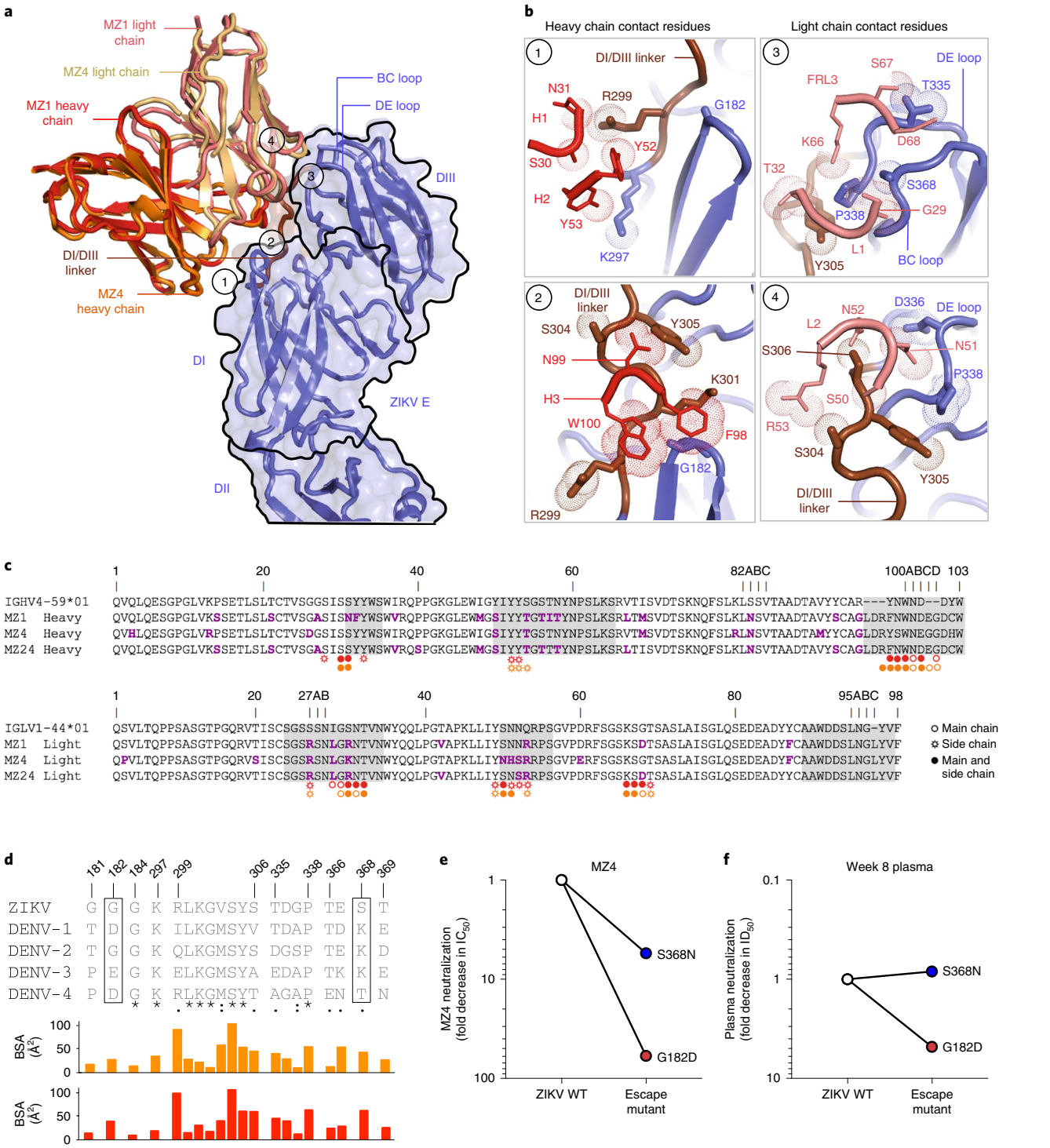

Fig. 2 | Crystal structure of human antibody MZ1 and MZ4 in complex with ZIKV E glycoprotein. a, Superimposition of the structures of MZ1-ZIKV E and MZ4-ZIKV E complexes. Antibodies MZ1 and MZ4 recognize the ZIKV E DI/DIII linker, DI and DIII domains. MZ1 (red) and MZ4 (orange) Fv domains are shown in ribbon representation, and ZIKV E (light blue) is shown in ribbon and transparent surface representation with the DI/DIII linker highlighted in dark brown. **b**, MZ1 and ZIKV E contact residues are shown in stick and dot representations based on (1) CDRs H1, and H2; (2) CDR H3; (3) CDR L1 and FR L3; (4) CDR L2 antibody contacting regions. All antibody residue numbering and CDR loops are designated using the Kabat numbering system. **c**, Sequence alignment of MZ4 family antibodies and precursor germline genes. Antibody residues that interact with ZIKV E are indicated (open circles denote antibody main chain-only contacts, open circles with rays denote antibody side-chain-only contacts and filled circles denote both main-chain and side-chain contacts (MZ1, red; MZ4, orange)). Antibody somatic mutations are highlighted in bold purple, CDRs are shaded gray, and antibody residue numbering is shown above the sequence alignment. **d**, Structure-based sequence alignment of ZIKV and DENV1–4 E residues (ZIKV E residue numbering) that interact with MZ1 and MZ4 antibodies. Symbols *, : and . denote identical, similar and less similar residues, respectively. BSA for ZIKV E contacting residues (MZ1, red; MZ4, orange) are shown as bar graphs. ZIKV E residues, identified as MZ4 escape mutants in **e**, are boxed. **e**, ZIKV (Paraiba_01) escape from MZ4 neutralization identified two variants with reduced neutralization sensitivity as determined in the plaque reduction neutralization test ($PRNT_{50}$). **f**, Participant A week 8 plasma neutralization of the ZIKV WT and escape variants revealed a reduction in neutralization capacity against the ZIKV G182D variant.

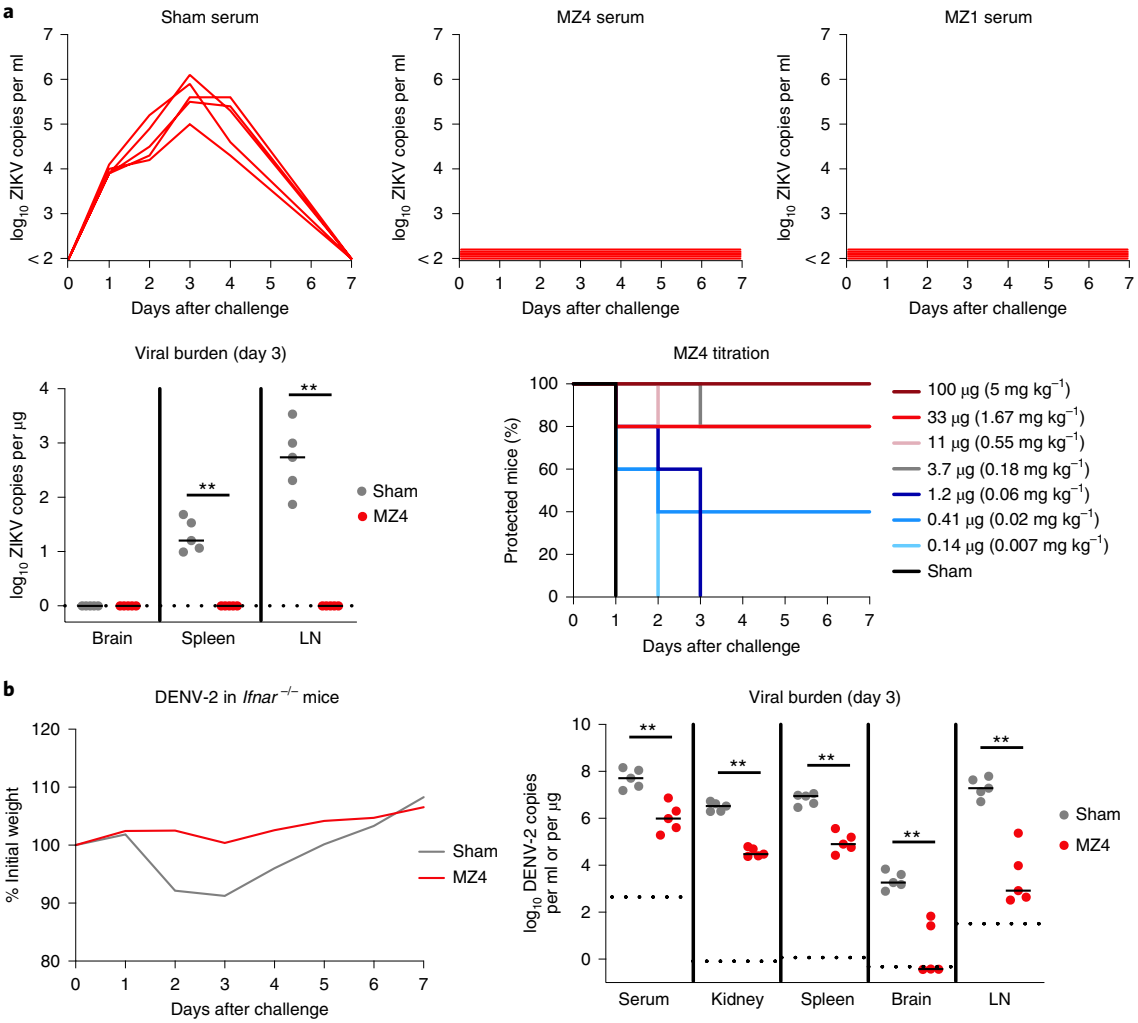

Fig. 3 | MZ4 protects mice in vivo from ZIKV and DENV-2 replication. a, Prophylaxis in a ZIKV replication mouse model. Antibodies were infused into groups of naive recipient wild-type (WT) Balb/c mice ($n=5$ per group) and challenged with 10^5 viral particles (10^2 plaque-forming units, p.f.u.) of ZIKV BR/2015. ZIKV viral loads were measured post-challenge by RT-PCR. Top: MZ4 and MZ1 afford complete protection from ZIKV replication at a single dose of 200 µg (10 mg kg^{-1}). Bottom left: a subset of mice ($n=5$ per group) were euthanized at day 3 and tissues were examined for the presence of ZIKV RNA. MZ4 prevented viral dissemination into the spleen and axillary lymph nodes (LN). Asterisks indicate significance from a two-tailed Mann–Whitney *t*-test, $P=0.0079$, $n=5$. Bottom right: in vivo titration of MZ4 prophylactic dose. Forty mice were infused with de-escalating doses of MZ4 ($n=5$ per dose). A Kaplan–Meier plot of MZ4 dose-dependent protective effects on ZIKV replication is shown. An ED_{50} of 2.55 µg (95% confidence interval (2.139, 3.262)) was calculated as the dose required to protect half of the animals using a five-parameter logistic regression analysis. **b**, Prophylaxis in a DENV-2 non-lethal weight loss mouse model. Antibodies were infused at a single dose of 200 µg into groups of naive *Ifnar*$^{-/-}$ C57BL/6 mice ($n=10$ per group) prior to DENV-2 S16803 challenge (10^6 p.f.u.). Mice were observed daily for weight loss and signs of clinical illness. Left: MZ4 protected mice from weight loss. Right: a subset of mice ($n=5$ per group) were euthanized on day 3 post-infection to examine tissues for the presence of DENV-2 RNA. MZ4 significantly reduced DENV-2 viremia and dissemination into the tissues. Asterisks indicate significance by two-tailed Mann–Whitney *t*-test, $P=0.0079$, $n=5$. Bars indicate median values. Dashed lines indicate the limit of detection of the assay.

sorting strategy with peripheral blood mononuclear cells (PBMCs) collected at week 8 (four weeks following the second vaccination) using a combination of fluorescently labeled whole ZIKV virions and ZIKV E and DENV-2 E glycoproteins (Extended Data Fig. 1). Antibody heavy and light chain V (D) J gene segments were amplified from single B cells using nested polymerase chain reaction with reverse transcriptase PCR (RT–PCR)[8–11] and sequenced. A total of 116 monoclonal antibodies (mAbs) were recovered and expressed as human IgG1, screened for binding to whole ZIKV and DENV-2 virions due to high neutralization titers against these viruses, and tested for neutralization in a microneutralization assay (MN)[6]. Eighty-three of the 116 mAbs bound to ZIKV or DENV-2 whole virions, and 66% of those were found to neutralize at least one DENV serotype (Fig. 1c and Extended Data Fig. 2). To examine the cross-neutralizing antibodies resulting from ZPIV vaccination, we focused on the six mAbs that were able to neutralize ZIKV and DENV1–4 with a 50% inhibitory concentration (IC_{50}) below 1 µg ml^{-1} (Fig. 1c–e and Extended Data Fig. 2). Sequence analysis revealed that those antibodies belonged to four different clonal families, with the VH4-59/VL1-44 family consisting of three members (MZ1, MZ4, MZ24) sharing similar complementarity-determining regions (CDR) H3 and L3 sequences (Fig. 1d). One of these mAbs, termed MHRP ZIKV-1004 (MZ4) demonstrated high neutralization potency against both ZIKV and DENV-2 with an IC_{50} of 8.3 and 20.9 ng ml^{-1}, respectively (Fig. 1e,f), on par with some of the most potent specific or cross-neutralizing ZIKV and DENV-2 mAbs identified so far[12–15] (Extended Data Fig. 3b–d). Potent activity against DENV-3 was also observed, as well as modest neutralization

against DENV-1 and -4 (Fig. 1g and Extended Data Fig. 3b). Although no neutralization activity was detected to WNV, YFV or JEV (Extended Data Fig. 3b), MZ4 had broad neutralization against ZIKV strains from American, Asian and African lineages (Extended Data Fig. 3e). Antibody-dependent enhancement of ZIKV, DENV-2 and DENV-3 infection was found using MZ4 in vitro using a concentration of less than 2 ng ml^{-1}, and was eliminated by introduction of the L_{234}A and L_{235}A (LALA) Fc mutations[16] (Extended Data Fig. 4).

Epitope-mapping experiments were next performed to delineate the epitope specificities of these antibodies. First, we measured binding activities against recombinant ZIKV and DENV-2 E proteins, as well as purified virions, to determine whether neutralizing epitopes were contained within quaternary or monomeric E protein conformations (Extended Data Fig. 5a–d). Antibodies from the MZ4 family bound better to ZIKV and DENV-2 virions than to their respective E proteins, suggesting that their epitopes contain quaternary characteristics (Extended Data Fig. 5b,d). Second, binding competition experiments showed that antibodies within the MZ4 family were only competed by the domain III (DIII)-directed antibody Z004 (ref. [15]), indicating that the epitope was within or overlapped with DIII (Fig. 1h). However, none of the MZ4 family members were able to bind to the recombinant ZIKV DIII (residues 303–404), suggesting that the epitope lies near but not within DIII (Extended Data Fig. 5e). Third, screening a comprehensive ZIKV prM/E alanine scan mutation library[17] identified the fusion loop as the target of antibodies MZ54 and MZ56, while MZ20 targeted DII (Fig. 1i and Extended Data Fig. 5f). The binding site of MZ4 family mAbs was identified as the ZIKV E DI/DIII linker region, revealing a novel cross-reactive epitope targeted through a conserved mode of recognition, with residues G302 and Y305 as critical components of the epitope (Fig. 1i and Extended Data Fig. 5f).

To understand the broad recognition of the MZ4 family antibodies, we determined the crystal structures of both MZ1 and MZ4 in complex with ZIKV E at a resolution of 4.2 and 4.3 Å, respectively (Fig. 2 and Extended Data Fig. 6). MZ1 and MZ4 bound to ZIKV DI and DIII centered on the DI/DIII linker region (residues 299–306) with buried surface areas (BSAs) of >350 Å^2 for both the antibody heavy and light chains (Fig. 2a,b and Supplementary Tables 1–3). MZ1 and MZ4 recognize ZIKV E in a highly similar manner with a root mean square deviation (r.m.s.d.) of 0.82 Å. Comparisons between the unbound Fab structures of MZ1, MZ4 and MZ24 showed a r.m.s.d. of 0.45 Å for the Fv regions, with the exception of three amino acids in the unbound structure of the MZ24 CDR H3 (Extended Data Fig. 6c,d). MZ4/MZ1 recognition of E is based on four structural elements (Fig. 2a–c and Extended Data Fig. 6). First, the CDR H1 and CDR H2 interacts with DI and the DI/DIII linker via a set of Tyr residues engaging the main chain atoms of ZIKV E G182 and the side chains of K297 and R299 (Fig. 2b, inset 1). Second, the CDR H3 binds to the full DI/DIII linker with ~300 Å^2 of BSA (296 Å^2 MZ1; 364 Å^2 MZ4), forming hydrogen bonds with R299, S304 and Y305, while also interacting with G182 of DI (Fig. 2b, inset 2). Third, the CDR L1 buries >125 Å^2 (141 Å^2 MZ1; 130 Å^2 MZ4) of DIII surface area, while the FR L3 interacts with the DIII BC- and DE-loops (Fig. 2b, inset 3). Fourth, the CDR L2 (residues 50–52) binds to the DI/DIII linker and DIII (Fig. 2b, inset 4). In agreement with the ZIKV alanine scan screening, the DI/DIII linker is critical for MZ4 family antibody interactions (Fig. 1i). MZ1 (7H bonds) and MZ4 (6H bonds) antibody heavy and light chains form extensive interactions with this region (Supplementary Tables 2 and 3). Modeling the MZ4-ZIKV E structure on the mature ZIKV virion[18] revealed potential quaternary contact sites at the pentamer vertex, and at the inter-raft interface, as indicated by the ZIKV virion/E binding assays (Extended Data Fig. 5b,d) without antibody clashes with adjacent E protomers (Extended Data Fig. 6e).

Despite the significant overall sequence variation seen in the E glycoprotein between ZIKV and the four DENV serotypes, residues within the MZ1/MZ4 epitope have high overall sequence similarity. However, a subset of residues within the epitope show meaningful differences between ZIKV/DENV serotypes, including residues 182, 299 and 306 (Fig. 2d). Viral escape analysis of ZIKV in the presence of MZ4 identified two separate escape mutations G182D and S368N, which led to significant reduction in MZ4 neutralization potency (Fig. 2e). Remarkably, G182D matched the natural viral sequence of DENV-1 and DENV-4 (Fig. 2d) and reduced susceptibility of these viruses to MZ4 neutralization (Fig. 1g). When tested against participant A week 8 plasma, the ZIKV G182D variant showed a 4.8-fold reduction in inhibitory dilution at 50% (ID_{50}) neutralization titer over ZIKV, suggesting that MZ4-like antibodies significantly contributed to the plasma neutralization after two ZPIV vaccinations (Fig. 2f).

To further understand MZ4 recognition, we compared the MZ4 epitope to epitopes within the same region of previously described ZIKV- or DENV-targeting antibodies[13,15,19–21] (Extended Data Fig. 7). Although the cross-neutralizing epitope recognized by the MZ4 family members is unique, the highest degree of epitope overlap was identified with mAb 5H2[22], a chimpanzee DENV-4-specific mAb (68% BSA). The 5H2 epitope, like MZ4, included several residues of the DI/DIII linker[19] (Extended Data Fig. 7), but is limited in breadth due to lower sequence homology within the DI region of its epitope.

Fig. 4 | A single ZPIV vaccination elicited potent MZ4-like antibodies. a–h, Identification and characterization of MZ2, an MZ4-like antibody isolated two weeks following the first vaccination in participant A. **a**, Sequence alignment of MZ2 and MZ4 antibodies and precursor germline genes. ZIKV E contact residues are indicated as in Fig. 2, with somatic mutations highlighted in bold purple. Residues that differ between MZ2 and MZ4 are underlined. **b**, Neutralization (FlowNT) of MZ2 against ZIKV and DENV1–4. **c**,**d**, Comparison of MZ2 and MZ4 neutralization potencies against ZIKV (Paraiba_01) (**c**) and DENV-2 (S16803) (**d**). Shown are the mean % neutralization obtained from two independent experiments with the IC_{50} (ng ml^{-1}) indicated in parentheses for each virus. **e**,**f**, MZ2 prevents ZIKV replication in serum (**e**) and tissues (**f**). Groups of naive recipient Balb/c mice ($n = 5$ per group) were treated with MZ2 (200 μg) and challenged with ZIKV as described in Fig. 3. Tissues were harvested at day 3 post-challenge. Asterisks indicate significance was reached using a two-tailed Mann–Whitney *t*-test, $P = 0.0079$, $n = 5$ mice. Bars indicate median value. **g**,**h**, Protective effect of MZ2 in a DENV-2 mouse model. MZ2 prevents weight loss (**g**) and significantly reduces viral burden in (**h**) serum and tissues. Groups of naive *Ifnar*$^{-/-}$ C57BL/6 mice ($n = 10$ per group) were treated with MZ2 (200 μg) and challenged with DENV-2 S16803 as described in Fig. 3. Dotted lines indicate the limit of detection of the assay, and the solid bars indicate the median DENV-2 viral burden. Asterisks indicate significance using a two-tailed Mann–Whitney *t*-test, $P = 0.0079$, $n = 5$ mice. **i**, Aggregate ZIKV geometric mean neutralization titers from ZPIV-vaccinated individuals in the Puerto Rico trial who had prior flavivirus exposure (red, $n = 34$) compared to flavivirus-naive (blue, $n = 20$) individuals enrolled in the Walter Reed Army Institute of Research (WRAIR) vaccine clinical trial. ZIKV neutralization titers were assessed and compared at baseline (week 0), four weeks following the first vaccination (week 4) or second vaccination (week 8) between each group. **j**, Comparison of ZIKV plasma microneutralization titers between flavivirus-naive (blue, five representative participants), flavivirus-experienced vaccinees from Puerto Rico (red, five representative participants) and participant A (black) at baseline (week 0), two weeks following the first vaccination (week 2) and four weeks following the second vaccination (week 8). Bars indicate geometric mean titers with 95% confidence intervals. **k**, Cross-neutralization titers against ZIKV, DENV1–4, WNV, JEV and YFV in the same flavivirus-experienced (left, $n = 5$) and flavivirus-naive (right, $n = 5$) vaccinated participants described in **j**. Dotted lines indicate the lower limit of detection of the assay.

The MZ4 epitope also partially overlapped with epitopes from DIII mAbs that target residues near the DI/DIII linker C terminus (Extended Data Fig. 7a–c). In agreement with this structural analysis, binding of MZ4 to ZIKV E was blocked by pre-incubation with DIII mAbs Z004 (ref. [15]), ZV-67[13] and ZKA190[14], and 5H2[19,22] to DENV-4 E. Minimal binding competition was observed with MZ4 using 3H5[21,23] or Ab513[20] to DENV-2 and -4, respectively, that had minimal epitope overlap (Extended Data Fig. 7d).

Passive protection studies were next performed to investigate whether antibodies targeting the DI/DIII linker would protect against ZIKV and DENV-2 replication in vivo. A single dose of 200 µg (10 mg kg^{-1}) of MZ4 or MZ1 fully protected mice from ZIKV viremia, in a previously described wild-type mouse model[6], where mice were challenged with 10^5 viral particles. The viral load peaked three to four days post-challenge within the sham control group, whereas viral replication was undetectable over the course

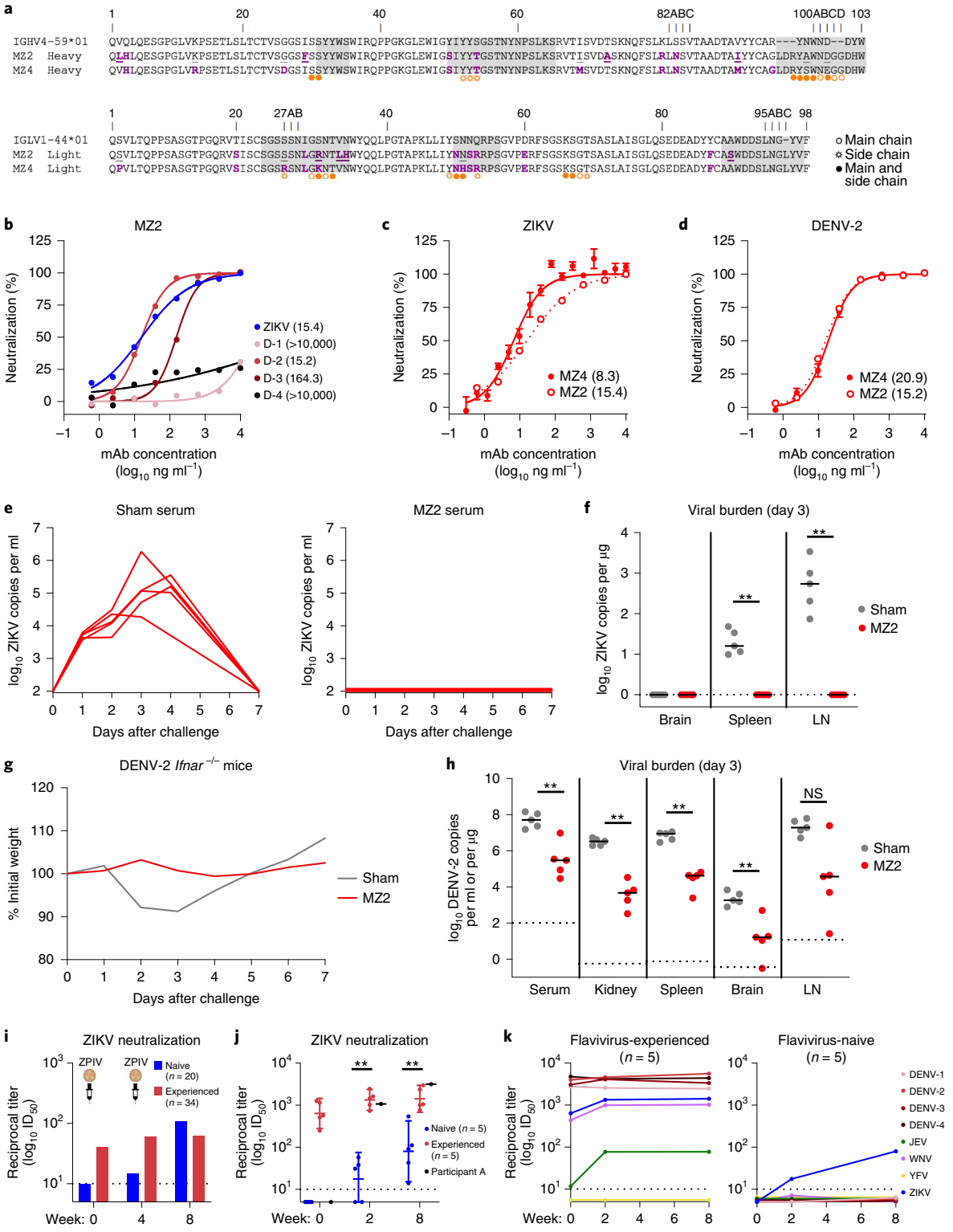

of the experiment when MZ4 or MZ1 was provided prophylactically (Fig. 3a, top). MZ4 also protected against viral dissemination into the brain, spleen and lymph nodes, while detectable RNA was found in the spleen and lymph nodes of the control mice (Fig. 3a, bottom left). To probe the minimal dose of MZ4 required for sterile protection, we titrated the MZ4 dose until protection was lost in 30 mice (Extended Data Fig. 8). Protection decreased gradually with the antibody dose yielding an effective dose at 50% (ED_{50}) of 2.55 µg (0.012 mg kg^{-1}) (Fig. 3a bottom right and Extended Data Fig. 8). In a DENV-2 *Ifnar*$^{-/-}$ non-lethal mouse model, MZ4 protected mice from weight loss and significantly reduced viral burden in the serum, kidney, spleen, brain and lymph nodes (Fig. 3b).

Because high binding and neutralizing titers were detected at week 2 following the first ZPIV vaccination, we sought to determine if these early neutralization responses were associated with the induction of MZ4-like antibodies. Therefore, we utilized the same B cell sorting strategy to isolate antigen-positive B cells two weeks following the first vaccination (Extended Data Fig. 1). Using this approach, we isolated a mAb with high sequence similarity to MZ4, identical CDR3 lengths, and heavy and light chain inferred precursor genes (Fig. 4a), which we called 'MZ2', for two weeks following the first vaccination. MZ2 yielded nearly identical binding, affinity and neutralization potency as MZ4 (Fig. 4b–d and Extended Data Fig. 9a–c), and targeted a similar epitope within the DI/DIII linker on ZIKV and DENV-2 (Extended Data Fig. 9d). In addition, MZ2 was able to protect against ZIKV and DENV-2 viremia and viral dissemination in mice (Fig. 4e–h). These data provide evidence that a single dose of ZPIV was sufficient to elicit cross-reactive neutralizing antibodies with the potential to protect against ZIKV and DENV-2 in participant A.

To determine how prior flavivirus exposure shaped the ZPIV-elicited responses, longitudinal plasma samples from participant A were analyzed for flavivirus binding and neutralization and compared to responses from ZPIV-vaccinated individuals without prior flavivirus exposure (Extended Data Fig. 10a,b). Although participant A elicited high-magnitude ZIKV and DENV-2 binding and neutralizing antibodies two weeks following a single vaccination (Extended Data Fig. 10a), flavivirus-naive donors who received the same ZPIV vaccine regimen demonstrated modest ZIKV binding and neutralization titers after the first vaccination, with no cross-reactivity to DENV-2 (Extended Data Fig. 10b). To determine if the ZPIV-elicited vaccine responses in flavivirus-experienced individuals were unique to participant A, we examined the immune responses from a set of flavivirus-experienced individuals from Puerto Rico who received the same ZPIV vaccination regimen (NCT03008122). Similar kinetics of ZIKV neutralization following vaccination were also observed in the flavivirus-experienced Puerto Rican individuals (Fig. 4i,j), where a single dose of ZPIV elicited high ZIKV neutralization titers. In addition to ZIKV neutralization, cross-neutralizing antibody responses against DENV-2, DENV-3, JEV and WNV were boosted following the first ZPIV dose (Fig. 4k) and maintained after the second ZPIV vaccination (Fig. 4k), similar to participant A. These results are in marked contrast to the flavivirus-naive individuals where cross-neutralizing antibody responses were absent (Fig. 4k).

In this study, we isolated potent ZIKV-DENV cross-neutralizing antibodies from three different B cell lineages, indicating that ZPIV vaccination was able to induce neutralizing responses through multiple genetic pathways. Biophysical mapping and structural characterization revealed that the most potent mAb, MZ4, targeted a novel epitope centered at the DI/DIII linker in both ZIKV and DENV-2. MZ4 belongs to a new class of ZIKV/DENV cross-neutralizing antibodies, adding to previously characterized cross-neutralizing epitopes such as the fusion loop epitope targeted by 2A10G6[24], the E dimer epitope[12] and the DIII lateral ridge epitope recognized by Z004 (ref. [15]). The MZ4 epitope is unique but overlaps with a previously identified chimpanzee DENV-4 specific mAb, 5H2[22]. Given the epitope overlap, it is likely that MZ4 binding to the DI/DIII linker prevents the structural rearrangements required for the formation of the fusogenic E trimer[25], thereby blocking membrane fusion in the endosome as demonstrated for 5H2[19]. MZ4 was exceptionally potent against ZIKV and DENV-2, with an IC_{50} on par with the most potent ZIKV and DENV-2 specific mAbs described so far. In vivo, animal challenge studies demonstrated that MZ4 protected mice from viremia and viral dissemination following ZIKV and DENV-2 challenge. The therapeutic potential of MZ4 can be further enhanced by introduction of the LALA mutation, to minimize antibody-dependent enhancement, and possible combination with mAbs of different specificities to prevent viral escape.

MZ2, an antibody with similar potency and characteristics as MZ4, was isolated following the first vaccination, suggesting that a single immunization was sufficient to elicit these potent cross-reactive antibodies. Such a rapid appearance suggests that MZ4 originated from a DENV-primed memory B cell recalled upon ZIKV vaccination. We were, however, not able to recover any MZ4-like antibodies prior to ZPIV vaccination by performing the same B cell sorting on week 0 PBMCs from participant A. If MZ4-like encoding memory B cells were present in the periphery prior to vaccination, their low frequency prevented isolation using our current methods. Further studies are needed to determine the ontogeny of this antibody lineage.

ZPIV vaccination also elicited neutralization responses of similar magnitude after a single ZPIV vaccination in flavivirus-experienced individuals from Puerto Rico, indicating that the kinetics of this type of response characterized in participant A could be reproducibly elicited in other flavivirus-primed individuals. These results indicate that a single ZPIV vaccination in individuals with prior exposure to DENV may induce an antibody response that mediates protection against both ZIKV and DENV-2 infection. Furthermore, the beneficial effects of prior DENV exposure described here in the context of vaccination could offer mechanistic insights into the recent finding that pre-existing, high antibody titers to DENV were associated with reduced risk of ZIKV infection and symptoms in a large Brazilian prospective cohort[26]. The implications of this study are that ZIKV vaccination can boost existing DENV responses while generating potent ZIKV-neutralizing responses and may have unique potential as a preventative strategy in settings where both viruses are prevalent.

Online content

Any methods, additional references, Nature Research reporting summaries, source data, extended data, supplementary information, acknowledgements, peer review information; details of author contributions and competing interests; and statements of data and code availability are available at https://doi.org/10.1038/s41591-019-0746-2.

Received: 18 January 2019; Accepted: 18 December 2019;
Published online: 3 February 2020

References

1. Barouch, D. H., Thomas, S. J. & Michael, N. L. Prospects for a Zika virus vaccine. *Immunity* **46**, 176–182 (2017).
2. Morabito, K. M. & Graham, B. S. Zika virus vaccine development. *J. Infect. Dis.* **216**, S957–S963 (2017).
3. Pierson, T. C. & Diamond, M. S. The emergence of Zika virus and its new clinical syndromes. *Nature* **560**, 573–581 (2018).
4. Abbink, P. et al. Protective efficacy of multiple vaccine platforms against Zika virus challenge in rhesus monkeys. *Science* **353**, 1129–1132 (2016).
5. Abbink, P. et al. Durability and correlates of vaccine protection against Zika virus in rhesus monkeys. *Sci. Transl. Med.* **9**, eaao4163 (2017).
6. Larocca, R. A. et al. Vaccine protection against Zika virus from Brazil. *Nature* **536**, 474–478 (2016).

7. Modjarrad, K. et al. Preliminary aggregate safety and immunogenicity results from three trials of a purified inactivated Zika virus vaccine candidate: phase 1, randomised, double-blind, placebo-controlled clinical trials. *Lancet* **391**, 563–571 (2018).
8. Tiller, T. et al. Efficient generation of monoclonal antibodies from single human B cells by single cell RT-PCR and expression vector cloning. *J. Immunol. Methods* **329**, 112–124 (2008).
9. Liao, H. X. et al. High-throughput isolation of immunoglobulin genes from single human B cells and expression as monoclonal antibodies. *J. Virol. Methods* **158**, 171–179 (2009).
10. Wu, X. et al. Rational design of envelope identifies broadly neutralizing human monoclonal antibodies to HIV-1. *Science* **329**, 856–861 (2010).
11. Doria-Rose, N. A. et al. Developmental pathway for potent V1V2-directed HIV-neutralizing antibodies. *Nature* **509**, 55–62 (2014).
12. Barba-Spaeth, G. et al. Structural basis of potent Zika-dengue virus antibody cross-neutralization. *Nature* **536**, 48–53 (2016).
13. Zhao, H. et al. Structural basis of Zika virus-specific antibody protection. *Cell* **166**, 1016–1027 (2016).
14. Wang, J. et al. A human bi-specific antibody against Zika virus with high therapeutic potential. *Cell* **171**, 229–241 (2017).
15. Robbiani, D. F. et al. Recurrent potent human neutralizing antibodies to Zika virus in Brazil and Mexico. *Cell* **169**, 597–609 (2017).
16. Chappel, M. S. et al. Identification of the Fc gamma receptor class I binding site in human IgG through the use of recombinant IgG1/IgG2 hybrid and point-mutated antibodies. *Proc. Natl Acad. Sci. USA* **88**, 9036–9040 (1991).
17. Davidson, E. & Doranz, B. J. A high-throughput shotgun mutagenesis approach to mapping B-cell antibody epitopes. *Immunology* **143**, 13–20 (2014).
18. Sirohi, D. et al. The 3.8 Å resolution cryo-EM structure of Zika virus. *Science* **352**, 467-–4470 (2016).
19. Cockburn, J. J. et al. Structural insights into the neutralization mechanism of a higher primate antibody against dengue virus. *EMBO J.* **31**, 767–779 (2012).
20. Robinson, L. N. et al. Structure-guided design of an anti-dengue antibody directed to a non-immunodominant epitope. *Cell* **162**, 493–504 (2015).
21. Renner, M. et al. Characterization of a potent and highly unusual minimally enhancing antibody directed against dengue virus. *Nat. Immunol.* **19**, 1248–1256 (2018).
22. Men, R. et al. Identification of chimpanzee Fab fragments by repertoire cloning and production of a full-length humanized immunoglobulin G1 antibody that is highly efficient for neutralization of dengue type 4 virus. *J. Virology* **78**, 4665–4674 (2004).
23. Gentry, M. K., Henchal, E. A., McCown, J. M., Brandt, W. E. & Dalrymple, J. M. Identification of distinct antigenic determinants on dengue-2 virus using monoclonal antibodies. *Am. J. Trop. Med. Hyg.* **31**, 548–555 (1982).
24. Dai, L. et al. Structures of the Zika virus envelope protein and its complex with a flavivirus broadly protective antibody. *Cell Host Microbe* **19**, 696–704 (2016).
25. Lu, X. et al. Double lock of a human neutralizing and protective monoclonal antibody targeting the yellow fever virus envelope. *Cell Rep.* **26**, 438–446 e435 (2019).
26. Rodriguez-Barraquer, I. et al. Impact of preexisting dengue immunity on Zika virus emergence in a dengue endemic region. *Science* **363**, 607–610 (2019).

Methods

ZPIV clinical studies. Monoclonal antibodies were isolated from a flavivirus-experienced participant (participant A) enrolled in the Z001 Zika purified inactivated virus (ZPIV) phase 1 vaccine clinical trial (NCT02937233) conducted at Beth Israel Deaconess Medical Center (BIDMC). Participant A is a US resident originally born in a flavivirus-endemic area that did not report any clinical history of flavivirus infection or receipt of a flavivirus vaccination. Participant A did report traveling back to their origin of birth every few years, but not in the five years preceding enrollment of the trial. Flavivirus-naive plasmas were obtained from participants enrolled in the WRAIR 2350 (RV478) ZPIV phase 1 vaccine clinical trial (NCT02963909) conducted at Walter Reed Army Institute of Research (WRAIR). Plasma from flavivirus-experienced individuals was obtained from study 16-0034 (NCT03008122), a phase I study conducted in Puerto Rico to evaluate the safety and immunogenicity of ZPIV in individuals from a flavivirus endemic area. All participants were vaccinated with 5 µg of ZPIV formulated with aluminum hydroxide gel adjuvant on days 1 (week 0) and 29 (week 4), as previously described[7]. For further evaluation of flavivirus cross-neutralization, five individuals were randomly selected from the Puerto Rican (NCT03008122) and WRAIR (NCT02963909) ZPIV clinical trials based upon prior flavivirus exposure using a panel of flavivirus microneutralization assays. For the Puerto Rican flavivirus-experienced individuals, five individuals were randomly selected with confirmed flavivirus exposure prior to ZPIV vaccination as determined by microneutralization. Similarly, for the flavivirus-naive WRAIR individuals, individuals were selected who tested negative to other flaviviruses via neutralization at baseline prior to ZPIV vaccination. All authors have complied with the ethical regulations regarding these studies. The studies were approved by the BIDMC, WRAIR, St Louis University and Quorum Central (now Advarra Central) Institutional Review Boards, and written informed consent was obtained from all participants. Please see the Life Sciences Reporting Summary for further information on these clinical trials.

Preparation of viruses. Unless otherwise indicated, all viruses used in this study were produced from C6/36 mosquito cells. Briefly, C6/36 cells were grown in T75 flasks and infected with ZIKV (Paraiba_01, GenBank KX280026), DENV-1 (WestPac74, GenBank U88535), DENV-2 (S16803, GenBank GU289914), DENV-3 (CH53489, GenBank DQ863638) or DENV-4 (TVP360, GenBank KU513442) at a multiplicity of infection of ~0.1 p.f.u. per cell. Infected cell culture supernatants were collected on day 5 post-infection. Viruses were pelleted by ultracentrifugation on a 30% sucrose cushion and resuspended in phosphate-buffered saline (PBS). The purity of the viral preparations was verified by sodium dodecyl sulfate–polyacrylamide gel electrophoresis (SDS–PAGE). For the microneutralization assay, ZIKV (PRVABC59, GenBank KX087101), DENV-1 (WestPac74), DENV-2 (S16803), DENV-3 (CH53489), DENV-4 (TVP360), JEV (SA14-14-2), WNV (4Delta30-Sw#134) and YFV (17-D) were passaged in Vero cells at least once. Viral supernatants were clarified, filtered, stabilized in 50% FBS and stored at −80 °C in single use aliquots.

Sorting of ZIKV-positive B cells. PBMCs from participant A were collected prior to ZPIV vaccination (week 0), two weeks after the first vaccination (week 2) and four weeks following the second ZPIV vaccination (week 8). PBMCs were also obtained from known ZIKV-naive participants at week 0 enrolled in the WRAIR ZPIV phase 1 vaccine clinical trial described above where individuals were tested for prior ZIKV exposure by ZIKV neutralization assays at baseline. Cryopreserved PBMCs were thawed in warm medium containing benzonase, then washed with PBS and stained for viability using Invitrogen Aqua Live/Dead stain. Cells were incubated at 4 °C for 30 min with a cocktail of antibodies including CD3 BV510 (BD Biosciences), CD4 BV510 (BD Biosciences), CD8 BV510 (BioLegend), CD14 BV510 (BioLegend), CD16 BV510 (BD Biosciences) and CD56 BV510 (BioLegend) as dump channel markers, and CD19 ECD (Beckman Coulter), IgG BV785 (BioLegend), IgD APC-Cy7 (BioLegend) and IgM PE-Cy5 (BD Biosciences). ZIKV E and DENV-2 E were tetramerized and conjugated to BV421 (BioLegend) and BV650 (BioLegend), respectively. To obtain monoclonal antibodies that target quaternary epitopes, primary staining also included live whole ZIKV virions (Paraiba_01) followed by secondary staining using 4G2[27] (Biovest) conjugated to APC (Thermofisher). FlowJo version 9.9.6 was used for data analysis and generation of the flow plots. See Extended Data Fig. 1 for the gating strategy. $CD19^+/IgG^+/IgD^-/IgM^-$ B cells reactive to ZIKV-E, DENV-E or whole ZIKV virions were sorted directly into lysis buffer (murine RNAse inhibitor (New England Biolabs), dithiothreitol (DTT) and SuperScript III First Strand Buffer (ThermoFisher), Igepal (Sigma) and carrier RNA (Qiagen) at one cell per well into PCR plates using a FACSAria (Becton Dickinson) and stored at −80 °C until subsequent reverse transcription. We focused on sequencing and cloning B cell receptors (BCRs) from DENV-2 E positive B cells with and without cross-reactivity with ZIKV E or whole ZIKV virions. The same sorting strategy was performed from PBMCs obtained from participant A at week 0, prior to ZPIV vaccination, to determine if MZ4 family members were present prior to vaccination, and at week 2, two weeks following first ZPIV vaccination, where high neutralization titers against ZIKV and the four DENV serotypes were observed. Sorting at week 8 with a comparable numbers of B cells was performed on a different day compared to PBMCs from participant A at week 0 and week 2, and the ZIKV-naive donor. Increased frequencies of antigen-specific and cross-reactive B cells were detected against all antigens (whole ZIKV virions, ZIKV E and DENV-2 E) between week 0 and week 2 (Extended Data Fig. 1b).

Antibody sequencing and production. RNA from single B cells was reverse-transcribed using random hexamers and the SuperScriptIII kit (ThermoFisher). Antibody V (D) J genes were amplified from the cDNA by nested PCR, using a HotStar Taq DNA Polymerase kit (Qiagen) and a combination of primer sets and methods as described previously[8–11]. V (D) J gene assignment, somatic hypermutation and CDR3 determinations were performed using IgBlast[28]. Antibody variable regions were synthesized and cloned (Genscript) into CMVR expression vectors (NIH AIDS reagent program) between a murine Ig leader (GenBank DQ407610) and the constant regions of human IgG1 (GenBank AAA02914), Igκ (GenBank AKL91145) or Igλ (GenBank AAA02915). Plasmids encoding heavy and light chains were co-transfected into Expi293F cells (ThermoFisher) according to the manufacturer's instructions. After five days, antibodies were purified from cleared culture supernatants with protein-A agarose (ThermoFisher) using standard procedures, buffer exchanged into PBS and quantified from A_{280} measurements. The purity and stability of the monoclonal antibodies were assessed by SDS–PAGE and Coomassie staining in both reducing and non-reducing conditions. Control antibodies 2A10G6[24], EDE1-C8 and EDE2-A11[12,29], Z3L1[30], Z004[15], ZV-67[13], ZKA190[14], Ab513[20], 2D22[31] and VRC01[10] were all expressed as human IgG1 and purified from Expi293F cells, as described above. 3H5 was provided by Harlan (now Envigo) and produced using a hybridoma cell line[23].

Fab production. Endoproteinase LysC (from New England BioLabs) at a ratio of 1:2000 (wt/wt) was incubated with MZ antibodies in PBS buffer (pH 7.4). Reaction was allowed to proceed for 3–5 h in a shaker incubator at 37 °C with 100 r.p.m. shaking speed. Digestion was assessed by SDS–PAGE and, upon completion, the reaction mixture was passed through protein-A beads (0.5–1 ml beads) three times and the final flowthrough was assessed by SDS–PAGE for purity.

Production of recombinant proteins. Recombinant ZIKV soluble E protein (1–404) from strain PRVABC59 (GenBank KX087101) and DENV-2 E (1–396) from strain 16681-PDK53 (GenBank M84728) were produced with C-terminal AviTag and poly-histidine tags from Expi293F cells. The coding sequence for prM/E was synthesized (Genscript) and cloned into the pcDNA3.4 vector (ThermoFisher) downstream from a murine Ig leader sequence. Following transient co-transfection with a furin (GenBank BC012181) expression vector, mature E proteins were purified from cell culture supernatants using a Ni-NTA (Qiagen) affinity column. An isolated E domain III (303–404) was expressed by deleting the prM and domains I–II from the full-length prM/sE pcDNA3.4 construct. A cleavable twin-strep-tagged ZIKV E version as well as a DENV-4 soluble E protein were also expressed from stably transfected S2 cells using the Drosophila expression system from ThermoFisher according to the manufacturer's instructions. Briefly, DNA fragments encoding the first 405 residues of E from strain PRVABC59 and the first 396 residues of DENV-4 E (GenBank AER00190) were synthesized (Genscript) with either a C-terminal human rhinovirus 3c protease (HRV-3c) cleavage site followed by a twin-strep tag (IBA) or a C-terminal AviTag and poly-histidine tags, respectively, and cloned into the pMT-BiP vector (ThermoFisher). S2 cells were co-transfected with the respective pMT-BiP expression vector and the pCoBlast selection vector at a 19:1 (wt/wt) ratio. Stably transfected cells were selected with Blasticidin and adapted to suspension and serum-free medium (Lonza Insect Xpress). Expression was induced with 0.5 mM $CuSO_4$ and culture supernatants were harvested after seven days. The insect-produced ZIKV E was purified on a StrepTactin XT column (IBA) following the manufacturer's instructions and by gel filtration on an ENrich SEC 650 column (Bio-Rad) or GE Sephadex S200 column to obtain pure monomeric ZIKV E proteins. The DENV-4 E protein was purified using a Ni-NTA (Qiagen) affinity column.

Cell lines. D1-4G2-4-15 mouse hybridoma (ATCC #HB-112), C6/36 (ATCC #CRL-1660), Vero (ATCC #CCL-81), Expi293F (ThermoFisher Scientific #A14527), DS-2 (ThermoFisher Scientific #R69007), U937-DC-SIGN (ATCC #CRL-3253) and K562 (ATCC #CCL-243) cell lines were utilized in this study.

Biolayer interferometry. Real-time interactions between purified E proteins and antibodies were monitored on an Octet RED96 instrument (FortéBio). Avi-tagged recombinant ZIKV or DENV-2 E proteins, biotinylated with the BirA biotinylation kit (Avidity), diluted in kinetics buffer (0.1% (wt/vol) bovine serum albumin (BSA), 0.02% (vol/vol) Tween-20 in PBS; FortéBio) and immobilized on streptavidin (SA) biosensors (FortéBio) at ~50% of the sensor maximum binding capacity. Baseline was established in kinetics buffer. To measure Fab affinities, loaded biosensors were dipped into wells containing serial dilutions of the antibody Fab fragments for 450 s. ZIKV E:Fab complexes were then allowed to dissociate in buffer. After reference subtraction, apparent binding kinetic constants were determined from at least four concentrations of Fab by fitting the curves to a 1:1 binding model using the Data Analysis software 9.0 (FortéBio). For measurement

of plasma binding responses, loaded biosensors were dipped into wells containing plasma diluted at 1/40 in kinetic buffer for 900 s. The affinity of plasma polyclonal responses was estimated by measuring binding off-rates, as follows. Purified E proteins were loaded on SA biosensors at very low density (~5% of the sensor maximum binding capacity), followed by an association step of 1,800 s and a 3,600 s dissociation step in buffer. Off rates were calculated by fitting at least four dissociation curves obtained with a twofold dilution series of plasma to a 1:1 binding model.

Binding competition assays. The epitopes of the ZIKV-neutralizing mAbs were initially mapped by binding competition with a set of characterized control antibodies using biolayer interferometry (BLI). Sensors loaded with ZIKV E, DENV-2 E or DENV-4 E, as described above, were immersed into wells containing the first competing antibody at a concentration (ranging from 100 to 800 nM) necessary to reach binding saturation after 900 s. Next, biosensors were dipped into wells containing the second antibody, in the presence of the first competing antibody, and binding was measured after 900 s of association. The residual binding signal of the second antibody was expressed as a percentage of the maximum binding signal obtained in the presence of a non-binding control antibody (VRC01), run in parallel. As some competing antibodies did not reach saturation after the first 900 s association and continued to contribute to the binding signal together with the second antibody, a set of controls were run independently with all first competing antibodies alone for a 1,800 s association. The difference in signals obtained at $t = 1{,}800$ s and $t = 900$ s was subtracted from the signal obtained in the presence of the second antibody to generate a corrected residual binding signal. Antibodies were defined as competing when the binding signal of the second antibody was reduced to less than 30% of its maximum binding capacity, and non-competing when binding was greater than 70%. Intermediate competition was defined by binding levels of 30–70%. The HIV-1 specific VRC01 monoclonal antibody served as a negative control.

ELISA binding assays to ZIKV and DENV-2 whole virions and monomeric E glycoproteins. The binding of antibodies to whole ZIKV or DENV-2 viruses as described above was measured using a capture ELISA assay. ELISA plates were coated overnight at 4 °C with the capture antibody 4G2 at 100 ng per well in borate saline pH 9.0 buffer. After washes in PBS-T (PBS with 0.05% (vol/vol) Tween-20), plates were blocked with 1% (vol/vol) normal goat serum, 0.25% (wt/vol) BSA, 0.1% (vol/vol) Tween-20 for 30 min at 37 °C. Washes in PBS-T were performed after each subsequent step and all dilutions were made in blocking buffer. ZIKV and DENV were diluted and added at 50 µl per well and incubated for 2 h at 37 °C. Serial fourfold dilutions of antibodies starting at 20 µg ml^{-1} were added to the plate in duplicate and incubated for 2 h at 37 °C. Secondary horseradish peroxidase (HRP)-conjugated anti-human/simian IgG were added for 1 h at 37 °C and plates were developed using 3,3′,5,5′-tetramethylbenzidine (TMB) peroxidase substrate (KPL) and immediately read at 650 nm. The binding curves were fitted using a four-parameter logistic regression model in Prism 7 software (GraphPad). Values indicate mean binding responses calculated from two independent experiments.

Binding of antibodies to recombinant ZIKV or DENV-2 E proteins was also performed in a standard ELISA assay. ELISA plates were coated overnight at 4 °C with 100 ng of purified ZIKV or DENV-2 E (as described above) in sodium bicarbonate/carbonate pH 9.4 buffer. Plates were then blocked with 5% (wt/vol) nonfat dry milk, 1% (wt/vol) BSA in PBS for 1 h at 37 °C. Washes between each step were performed with 0.1% (vol/vol) Triton-X100 in PBS. Serial fourfold dilutions of antibodies starting at 20 µg ml^{-1} in 5% (vol/vol) FBS, 2% (wt/vol) BSA, 1% (vol/vol) Triton X100 in PBS were added to the plate in duplicate and incubated for 1 h at room temperature (RT). Secondary HRP-conjugated antibodies, substrate and data analysis were as described above for the whole virus ELISA. Values indicate mean binding responses calculated from two independent experiments.

Shotgun mutagenesis epitope mapping. Epitope mapping was performed by shotgun mutagenesis as described previously[17,32,33]. Briefly, ZIKV (SPH2015) and DENV-2 (16681) prM/E expression constructs were subjected to high-throughput alanine scanning mutagenesis to generate a comprehensive library of individual mutations where each residue within prM/E was changed to alanine, with alanine mutated to serine. MAb reactivities against each mutant prM/E clone were calculated relative to wild-type prM/E reactivity by subtracting the signal from mock-transfected controls and normalizing to the signal from wild-type prM/E-transfected controls. Mutations within clones were identified as critical to the mAb epitope if they did not support reactivity of the test mAb, but supported reactivity of other ZIKV mAbs. This counter-screen strategy facilitated the exclusion of prM/E mutants that are locally misfolded or have an expression defect. Residues from which substitution to alanine causes >60% loss in binding were considered important for binding.

Selection of MZ4 neutralization-resistant ZIKV variants. Based on previous experience, to quickly select for MZ4 neutralization-resistant variants and confirm the mapping of the MZ4 epitope, ZIKV was incubated with high concentrations of MZ4 before infection of Vero cell monolayers. Approximately 6 $\log_{10}$ p.f.u. of ZIKV virus (Paraiba_01, produced in Vero cells) were mixed with an equal volume of purified MZ4 at 50, 5, 0.5 and 0.05 µg ml^{-1} or medium-only control and incubated at 37 °C for 45 min. Following incubation, the mixtures were used to infect Vero cell monolayers in T25 flasks, which were incubated at 37 °C in medium containing the respective concentration of MZ4 or medium only and observed daily for cytopathic effect (CPE). After observing CPE, the cell culture supernatant was harvested, and a standard plaque titration assay was performed in Vero cells. Two plaques each were picked from flasks with 50 µg ml^{-1} and 5 µg ml^{-1} of MZ4 after the first passage. The plaque purified viruses were passaged once in Vero cells to generate working stocks, which were sequenced and tested in neutralization assays with MZ4 in comparison with the virus passage control. Of the four viruses sequenced after the first passage, one contained the envelope G182D mutation and three had the S368N mutation, including the two viruses isolated from the flask with 5 µg ml^{-1} of MZ4.

Microneutralization. A high-throughput microneutralization (MN) assay was performed as previously described[6,7,34]. The pan flavivirus mAb 6B6-C1 (a gift from J.T. Roehrig) was used to detect ZIKV, JEV, WNV and YFV, while 4G2 was used for the DENV1–4 assays. Assays were validated using the following criteria: the average absorbance at 450 nm of three non-infected control wells had to be ≤0.5, and that of virus-only control wells had to be ≥0.9. The percent reduction of infection was calculated from normalized absorbance values, and the antibody concentration (ng ml^{-1}) at which 50% neutralization (IC_{50}) is observed was derived using a five-parameter logistic regression analysis performed with the N-Parameter Logistic Regression (nplr) R package version 0.1-7[35]. Reported IC_{50} values are geometric means calculated from at least two independent experiments.

Flow neutralization test (FlowNT). A flow cytometry-based assay was used to determine the neutralization activity of purified recombinant mAb and plasma, as previously described[36]. Neutralization curves of the aggregate data were graphed in Prism (version 7, GraphPad Software) using a four-parameter logistic regression analysis with the top and bottom of the curves constrained to 100 and 0, and error bars indicating the standard error of the mean (s.e.m.). Reported IC_{50} values were calculated using a five-parameter logistic regression analysis, as described for the MN assay and under Statistical Analysis. Data are presented as mean ± s.e.m. calculated from at least two independent experiments performed in triplicate.

Plaque reduction neutralization test (PRNT). Serial dilutions of mAbs were mixed with an equal volume of virus, produced in Vero cells, and incubated for 1 h at 37 °C followed by infection of Vero cell monolayers in triplicate. Plaques were visualized by staining with Neutral Red. Neutralization curves were graphed in Prism and reported IC_{50} values were calculated using a five-parameter logistic regression analysis, as described above.

ADE assay. In vitro antibody-dependent enhancement of infection was quantified as previously described[36]. The percent of infected cells are reported as fold-ADE relative to baseline percent infection of K562 cells. The HIV-1-specific mAb VRC01 served as negative control. MZ4 harboring the Fc mutations abolishing binding to Fcγ receptors[37] (MZ4 LALA) was generated by introducing the L234A and L235A mutations[16] in MZ4 heavy chain expression plasmid.

X-ray crystallography. All proteins were crystallized by hanging-drop vapor diffusion at 273 K. MZ1 Fab (7.5 mg ml^{-1}), MZ4 Fab (6.5 mg ml^{-1}), MZ24 Fab (8.0 mg ml^{-1}), MZ1-ZIKV E complex (5.0 mg ml^{-1}) and MZ4-ZIKV E complex (6.8 mg ml^{-1}) were screened for crystallization conditions using an Art Robbins Gryphon crystallization robot, 0.2 µl drops, and a set of 1,200 conditions. Crystal drops were observed daily using a Jan Scientific UVEX-PS with automated ultraviolet and bright-field drop imaging. Initial crystallization conditions were optimized manually in larger 1 µl drops, and crystals used for data collection grew in the following crystallization conditions: MZ1 Fab, 0.2 M ammonium sulfate, 0.1 M sodium acetate trihydrate (pH 4.6) and 25% (wt/vol) polyethylene glycol 4,000; MZ4 Fab, 0.2 M ammonium sulfate, 0.1 M HEPES (pH 7.5) and 25% (wt/vol) polyethylene glycol 3350; MZ24 Fab, 0.1 M citric acid/NaOH (pH 4.0), 1 M lithium chloride and 20% polyethylene glycol 6000; MZ1-ZIKV E complex, 0.06 M magnesium chloride, 0.1 M imidazole MES monohydrate (pH 6.5), 20% ethylene glycol and 10% polyethylene glycol 8000; MZ4-ZIKV E complex, 1.26 M ammonium sulfate, 0.1 M CHES/NaOH (pH 9.5) and 0.2 M sodium chloride.

Diffraction data collection and processing. Single crystals were transferred to mother liquor containing 22% glycerol and cryo-cooled in liquid nitrogen before data collection. Diffraction data were collected at the Advanced Photon Source (APS), Argonne National Laboratory beamlines and at the National Synchrotron Light Source II (NSLS-II). Diffraction data for MZ1 Fab and MZ4 Fab were collected at APS 19-ID beamline to a final resolution of 2.05 Å and 2.95 Å, respectively, using a Q315r charge-coupled device (CCD) detector. Diffraction data for MZ1-ZIKV E crystals were collected at APS 24-ID-E beamline and measured using a Dectris Eiger 16M PIXEL detector to a final resolution of 4.2 Å. Diffraction data for MZ4-ZIKV E complex were collected at APS 19-BM beamline and measured using an ADSC Quantum 210r CCD detector to a final resolution of 4.3 Å. MZ24 Fab diffraction data were collected at beamline NSLS-II AMX 17-ID-1

and measured using an Eiger 9M PIXEL detector to a final resolution of 2.11 Å. MZ24 Fab data reduction and scaling were carried out with the XDS-based automated data processing pipeline, DIMPLE, at the beamline. For all other crystals, diffraction data indexing, integration and scaling were carried out using the HKL2000 suite[38]. Data collection statistics are reported in Supplementary Table 1.

Structure solution and refinement. Phenix xtriage was used to analyze all the scaled diffraction data output from HKL2000, suite37 and XDS (version 26 January 2018 BUILT=20180126). Primarily, data were analyzed for measurement value significance, completeness, asymmetric unit volume and possible twinning and/or pseudotranslational pathologies. All crystal structures described in this study were solved by molecular replacement using the program Phaser, version 2.1[39]. All Fab datasets (MZ1, MZ4 and MZ24), diffracted to a resolution ranging from 2.05 Å to 2.95 Å, and phenix xtriage (version 1.11.1-2575-0000) did not identify any data quality issue. The Fv and Fc domains of EDE1-C8 Fab (PDB code 4UTA), were used to solve the crystal structure of MZ1 Fab. The MZ1 Fab structure was used to solve the crystal structures of MZ4 and MZ24 Fabs. Diffraction data for the MZ1-ZIKV E and MZ4-ZIKV E complexes were significantly anisotropic, and were corrected using the UCLA Diffraction Anisotropy Server[40] prior to structure solution. Phenix xtriage did not identify any data quality issues for the MZ1-ZIKV E diffraction data except anisotropic diffraction. However, diffraction data for the MZ4-ZIKV E complex crystal was significantly anisotropic and also showed twinning pathology. Phenix xtriage suggested seven possible twin laws for this dataset. Data for the MZ4-ZIKV E complex were analyzed conservatively in space group *P*1 without using the suggested twin laws to avoid an artificial drop in the R_{free} value. To determine the structure of the Fab-ZIKV E structures, we divided ZIKV E (PDB code 5IRE) into smaller domains (DI, DII and DIII), and the MZ1/MZ4 Fab into Fv and Fc domains, and used a sequential search procedure. This approach was critical in finding a solution for both complexes. Refinement for all structure models was carried out using Phenix refine with positional, global isotropic B-factor refinement and defined translation/libration/screw (TLS) groups. Manual model building was performed in Coot. The final stages of refinement were performed with release of all non-crystallographic symmetry (NCS) restraints. Structure quality was assessed with MolProbity (Phenix version 1.11.1-2575-0000)[41]. The final refinement statistics for all structures are presented in Supplementary Table 1. The Ramachandran statistics for the atoms in favored, allowed and disallowed regions are as follows: MZ1 Fab, 96.0, 4.0, 0.0; MZ4 Fab, 95.0, 5.0, 0.0; MZ24 Fab, 97.0, 3.0, 0.0; MZ1-ZIKV E, 95.0, 5.0, 0.0; MZ4-ZIKV E, 96.0, 4.0, 0.0. In addition, based on the R_{free} values, we compared our structures to all structures with similar diffraction resolution in the PDB database. Based on this comparison, the R_{free} values for four of the structures had high percentile values (MZ1 Fab, 87.5; MZ4 Fab, 76.4; MZ24 Fab, 94.4; MZ1-ZIKV E, 97.0). The MZ4-ZIKV E complex structure, was at the ninth percentile, likely due to the significant anisotropy and twinning pathology of the crystal, and the inability to locate and model the Fc1 regions of the MZ4 Fab molecules. The percentile values for each structure are reported in Supplementary Table 1. PDB chains Z (ZIKV E), H (antibody heavy chain) and L (antibody light chain) were used for the structure analysis for both MZ1-ZIKV E and MZ4-ZIKV E structure complexes. Electron density $2F_o–F_c$ maps for the MZ1-ZIKV E and MZ4-ZIKV E contact regions are shown in Extended Data Fig. 6. MZ1-ZIKV E and MZ4-ZIKV E contact residues (Fig. 2 and Supplementary Tables 2 and 3), and previously described flavivirus-neutralizing antibody-E contact residues (Extended Data Fig. 7) were identified using PISA (PDBePISA version 1.52(20/10/2014))[42]. R.m.s.d. values for the structures of MZ1 and MZ4 in complex with ZIKV E were calculated using PyMOL (version 1.3). The MZ1-ZIKV E structure was aligned to MZ4 Fv in the MZ4-ZIKV E crystal structure to calculate the r.m.s.d. (Fig. 2a). All structure figures were generated using PyMOL (version 1.3; The PyMOL Molecular Graphics System, DeLano Scientific).

In vivo protection studies for ZIKV. In vivo passive protection experiments using MZ4 were performed on three separate occasions with ZIKV challenge using six- to eight-week-old female Balb/c mice, as previously reported[6]. Briefly, the indicated human monoclonal antibodies were infused intravenously into groups of naive recipient Balb/c mice ($n=5$ per group) prior to ZIKV-BR (GenBank KU497555.1) challenge. Mice received 100 µl (200 µg) of a 2 mg ml^{-1} solution of purified monoclonal antibody. To get an idea of the in vivo potency, 40 mice were used in a passive protection experiment with decreasing doses of MZ4 using a threefold dilution from 100 µg (5 mg kg^{-1}) to 0.14 µg (0.07 mg kg^{-1}). Two hours after infusion, mice were challenged with 10^5 viral particles (10^2 p.f.u.) of ZIKV BR/2015 intravenously. RT–PCR assays were utilized to monitor viral loads, as previously described[6], in plasma and tissues. To examine protection from viral dissemination into tissues, mice were euthanized at peak viremia (day 3) and the indicated tissues were harvested. RNA was extracted with a QIAcube HT (Qiagen). Serum samples were extracted using the Qiacube 96 Cador pathogen HT, and tissue samples were lysed in Qiazol using a Tissuelyser II (Qiagen), chloroform treated and extracted with the Qiacube 96 RNeasy HT kit. The wild-type ZIKV BeH815744 Cap gene was utilized as a standard. RNA standards were generated using the AmpliCap-Max T7 High Yield Message Maker Kit (Cell Script) and purified with an RNA clean and concentrator kit (Zymo Research). RNA quality and concentration were assessed by the BIDMC Molecular Core Facility. Log dilutions of the RNA standard were reverse-transcribed and included with each RT–PCR assay. RT–PCR was run on the Quantstudio 6 Flex (Applied Biosystems). Viral loads were calculated as virus particles (VP) per milliliter or VP per microgram of total RNA as measured on the NanoDrop (Thermo Scientific). The assay sensitivity was >100 copies per ml and >1 copy per µg total RNA. This study was approved by the Institutional Animal Care and Use Committee (IACUC), and research was conducted in compliance with the Animal Welfare Act and other federal statutes and regulations relating to animals.

In vivo protection studies for DENV-2. *Ifnar*$^{-/-}$ C57BL/6 female mice were obtained from Jackson Laboratories and used for DENV-2 infection studies. In this non-lethal mouse model, cohorts of 10 *Ifnar*$^{-/-}$ mice (five weeks of age) were infected with 6.7 $\log_{10}$ p.f.u. of DENV-2 strain S16803 by intraperitoneal injection. This dose and strain were previously shown to cause a significant amount of weight loss in *Ifnar*$^{-/-}$ mice compared to other evaluated DENV-2 strains (data not shown). To evaluate the efficacy of the monoclonal antibodies MZ2 and MZ4 in this DENV-2 weight loss model, three groups of 10 mice each received treatment with 200 µg of MZ2, MZ4 or vehicle control by subcutaneous injection 4 h prior to virus exposure with 6.7 $\log_{10}$ p.f.u. of DENV-2 strain S16803 by intraperitoneal injection. Mice were observed daily for weight loss and signs of clinical illness. A subset of mice ($n=5$ per group) were deeply anesthetized for blood sampling using cardiocentesis on day 3 post-infection to determine viremia followed by euthanasia to collect the following tissues for virus dissemination: kidney, liver, spleen, brain and axillary lymph node. DENV in sera and homogenized tissues was determined as previously described[43], with modification (the DENV-2 probe fluorophore was changed to JOE). RNA was extracted using the MagMax-96 Viral RNA isolation kit (Applied Biosystems) on the Kingfisher Flex Purification System (ThermoFisher Scientific). Eluted RNA was quantified by quantitative RT–PCR (qRT–PCR) using the SuperScript III Platinum One-Step qRT–PCR kit (ThermoFisher Scientific) on a QuantStudio 7-Flex Real-Time PCR instrument (ThermoFisher Scientific). DENV RNAemia was calculated as genome equivalents (GE) per milliliter using an internal standard curve of 10-fold serially diluted in vitro-transcribed RNA. The limit of quantitation defined here as detection of a standard curve dilution in ≥95% of at least 20 replicate curves tested, is 50 genome equivalents (GE) per reaction.

Statistical analysis. Binding experiments are presented as the mean values ± s.e.m. calculated from two independent experiments. Neutralization is the geometric mean of the IC_{50} values calculated using five-parameter regression from at least two independent experiments performed in triplicate. A Wilcoxon paired signed rank test was performed to verify the existence of significant differences in antibody neutralization activities between week 0 and week 2 antibody responses. A five-parameter logistic regression[35] was used to calculate the MZ4 ED_{50} in the mouse experiment. The number of parameters was optimized simultaneously using nonlinear minimization given a sum of squared error functions. A Mann–Whitney *t*-test was used to verify the existence of significant differences in viral burden between sham and MZ4- or MZ2-treated mice for a given organ and also to examine the existence of significant differences in ZIKV neutralization titers between flavivirus-naive and -experienced vaccinees at weeks 2 and 8. All tests, except for the Mann–Whitney *t*-test (performed in Prism, version 8, GraphPad Software), were performed in R (version 3.5.1) and R studio (1.1.442). Data were graphed using Prism software (version 7, GraphPad Software).

Reporting Summary. Further information on research design is available in the Nature Research Reporting Summary linked to this article.

Data availability

The associated accession numbers for the coordinates and structure factors reported in this paper have the following Protein Data Bank IDs: 6MTX, 6MTY, 6NIP, 6NIU and 6NIS. The sequences for MZ4, MZ1, MZ2, MZ20, MZ24, MZ54, MZ56 heavy chains and MZ4, MZ1, MZ2, MZ20, MZ24, MZ54, MZ56 light chains have been deposited in GenBank under ID codes MN523667, MN523668, MN523669, MN523670, MN523671, MN523672, MN523673, MN523674, MN523675, MN523676, MN523677, MN523678, MN523679 and MN523680, respectively. The data that support the findings of this study are available from the corresponding authors upon request. The interim aggregate data of the ZPIV trial in Puerto Rico (NCT03008122) are available with permission from the Division of Microbiology and Infectious Disease, NIAID, NIH, as this is currently an active, ongoing Phase I study.

References

27. Henchal, E. A., Gentry, M. K., McCown, J. M. & Brandt, W. E. Dengue virus-specific and flavivirus group determinants identified with monoclonal antibodies by indirect immunofluorescence. *Am. J. Trop. Med. Hyg.* **31**, 830–836 (1982).
28. Ye, J., Ma, N., Madden, T. L. & Ostell, J. M. IgBLAST: an immunoglobulin variable domain sequence analysis tool. *Nucleic Acids Res.* **41**, W34–W40 (2013).

29. Dejnirattisai, W. et al. A new class of highly potent, broadly neutralizing antibodies isolated from viremic patients infected with dengue virus. *Nat. Immunol.* **16**, 170–177 (2015).
30. Wang, Q. et al. Molecular determinants of human neutralizing antibodies isolated from a patient infected with Zika virus. *Sci. Transl. Med.* **8**, 369ra179 (2016).
31. Gallichotte, E. N. et al. A new quaternary structure epitope on dengue virus serotype 2 is the target of durable type-specific neutralizing antibodies. *mBio* **6**, e01461–01415 (2015).
32. Sapparapu, G. et al. Neutralizing human antibodies prevent Zika virus replication and fetal disease in mice. *Nature* **540**, 443–447 (2016).
33. Cox, K. S. et al. Rapid isolation of dengue-neutralizing antibodies from single cell-sorted human antigen-specific memory B-cell cultures. *MAbs* **8**, 129–140 (2016).
34. Thomas, S. J. et al. A phase II, randomized, safety and immunogenicity study of a re-derived, live-attenuated dengue virus vaccine in healthy adults. *Am. J. Trop. Med. Hyg.* **88**, 73–88 (2013).
35. Commo, F. & Bot, B.M. nplr: N-parameter logistic regression. Version 0.1-7 https://CRAN.R-project.org/package=nplr (2016).
36. McCracken, M. K. et al. Impact of prior flavivirus immunity on Zika virus infection in rhesus macaques. *PLoS Pathog.* **13**, e1006487 (2017).
37. Hezareh, M., Hessell, A. J., Jensen, R. C., van de Winkel, J. G. & Parren, P. W. Effector function activities of a panel of mutants of a broadly neutralizing antibody against human immunodeficiency virus type 1. *J. Virology* **75**, 12161–12168 (2001).
38. Otwinowski, Z. & Minor, W. Processing of X-ray diffraction data collected in oscillation mode. *Methods Enzymol.* **276**, 307–326 (1997).
39. McCoy, A. J. et al. Phaser crystallographic software. *J. Appl. Crystallogr.* **40**, 658–674 (2007).
40. Strong, M. et al. Toward the structural genomics of complexes: crystal structure of a PE/PPE protein complex from *Mycobacterium tuberculosis*. *Proc. Natl Acad. Sci. USA* **103**, 8060–8065 (2006).
41. Chen, V. B. et al. MolProbity: all-atom structure validation for macromolecular crystallography. *Acta Crystallogr. D* **66**, 12–21 (2010).
42. Krissinel, E. & Henrick, K. Inference of macromolecular assemblies from crystalline state. *J. Mol. Biol.* **372**, 774–797 (2007).
43. Klungthong, C. et al. Monitoring and improving the sensitivity of dengue nested RT-PCR used in longitudinal surveillance in Thailand. *J. Clin. Virol.* **63**, 25–31 (2015).

Acknowledgements

We sincerely thank the clinical trial participants and staff. In addition, we thank M. Creegan, M. Eller and the MHRP FlowCore facility for help with FACS sorting and C. Kuklis, Q. Chen, D. Barvir, A. Srikanth, T. Li, C. Fung, B. Yadav, B. Sumlin, G. Ballarini, N. Burrell, R. Olson and A. Dean for technical support. X-ray diffraction data were collected at beamlines at the Advanced Photon Source, Argonne National Laboratory, and the National Synchrotron Light Source II. This work was primarily funded by the US Department of the Army and the Defense Health Agency (0130602D16) to K.M. Work at BIDMC under D.B. was performed with support from the US Department of Defense, Defense Health Agency (0130602D16), the Henry M. Jackson Foundation and the Harvard Catalyst, Harvard Clinical and Translational Science Center (National Center for Research Resources and the National Center for Advancing Translational Sciences, National Institutes of Health Award UL1 TR001102) and with financial contributions from Harvard University and its affiliated academic healthcare centers. The ZPIV vaccine trial in Puerto Rico was funded by the Vaccine Treatment Evaluation Unit (VTEU) at Saint Louis University (contract no. HHSN27220130000021I) under S.L.G. The network of VTEUs is supported by the National Institute of Allergy and Infectious Diseases, part of the National Institutes of Health. The funders of the clinical trials were involved in the clinical study design, clinical study operations and approval of the clinical protocols. The ZPIV program leads (K.M. and N.L.M.) and the study sponsors had final responsibility for the decision to submit for publication. This work was supported by a cooperative agreement (W81XWH-07-2-0067) between the Henry M. Jackson Foundation for the Advancement of Military Medicine and the US Department of Defense (DoD) under the leadership of N.L.M. and M.R. The Structural Biology Center (SBC) and Northeastern Collaborative Access Team (NE-CAT) beamlines are funded by the National Institute of General Medical Sciences from the National Institutes of Health (P41 GM103403) at the Advanced Photon Source, Argonne National Laboratory. SBC-CAT is operated by UChicago Argonne for the US Department of Energy, Office of Biological and Environmental Research under contract no. DE-AC02-06CH11357. This research used ID-17-1 (AMX) beamline of the National Synchrotron Light Source II, a US Department of Energy (DOE) Office of Science User Facility operated for the DOE Office of Science by Brookhaven National Laboratory under contract no. DE-SC0012704. In addition, this work was supported by NIH contract no. HHSN272201400058C to B.J.D. Material has been reviewed by the Walter Reed Army Institute of Research. The content is solely the responsibility of the authors and does not necessarily represent the official views of Harvard Catalyst, Harvard University and its affiliated academic healthcare centers or the National Institutes of Health. The opinions or assertions contained herein are the private views of the authors, and are not to be construed as official, or as reflecting true views of the Department of the Army or the Department of Defense. The investigators have adhered to the policies for protection of human subjects as prescribed in AR 70–25.

Author contributions

Conceptualization was provided by K.E.S., D.H.B., E.B., S.L.G., K.M., S.J.K., M.G.J. and N.L.M. Investigations were carried out by V.D., R.S.S., G.D.G., G.D., R.A.D.L.B., R.A.L., W.Z., L.M.-R., M.C., E.D., M.K.M., J.D.B., P.A., H.B., A.L.B., C.H.B., I.M.B., N.B., T.C., N.A.D.-R., A.G.i.E., J.A.F., A.G., M.H., B.S.H., N.J., K.K., D.J.L., J.L., A.K.P., W.R., I.S., U.T., S.T., M.G.J. and S.J.K. Data curation was performed by V.D., R.S.S., G.D.G., G.D., R.A.D.L.B., R.A.L., M.G.J. and S.J.K. The original draft was written by V.D., G.D., R.S.S., M.G.J. and S.J.K. Review and editing was carried out by all authors. Visualization was provided by V.D., R.S.S., G.D.G., G.D., R.A.L., M.G.J. and S.J.K. Supervision was provided by B.J.D., M.R., A.B.M., I.S.G., R.T., M.L.R., K.H.E., M.K., D.R.S., R.G.J., S.L.G., K.E.S., D.H.B., K.M., N.L.M., M.G.J. and S.J.K. Funding acquisition was carried out by M.L.R., R.G.J., B.J.D., D.H.B., K.M. and N.L.M.

Competing interests

B.J.D. is a shareholder of Integral Molecular. D.H.B. has received grants from Novavax and personal fees from IGM Biosciences. Patent application no. PCT/US19/28952 containing the mAbs described in this publication has been filed for authors S.J.K., N.L.M., V.D., D.H.B., K.M., R.G.J., R.S.S., G.D., M.G.J. and K.E.S. The status of the patent is pending, not yet published. The other authors declare no competing interests.

Additional information

Extended data is available for this paper at https://doi.org/10.1038/s41591-019-0746-2.

Supplementary information is available for this paper at https://doi.org/10.1038/s41591-019-0746-2.

Correspondence and requests for materials should be addressed to M.G.J. or S.J.K.

Peer review information Alison Farrell was the primary editor on this article and managed its editorial process and peer review in collaboration with the rest of the editorial team.

Reprints and permissions information is available at www.nature.com/reprints.

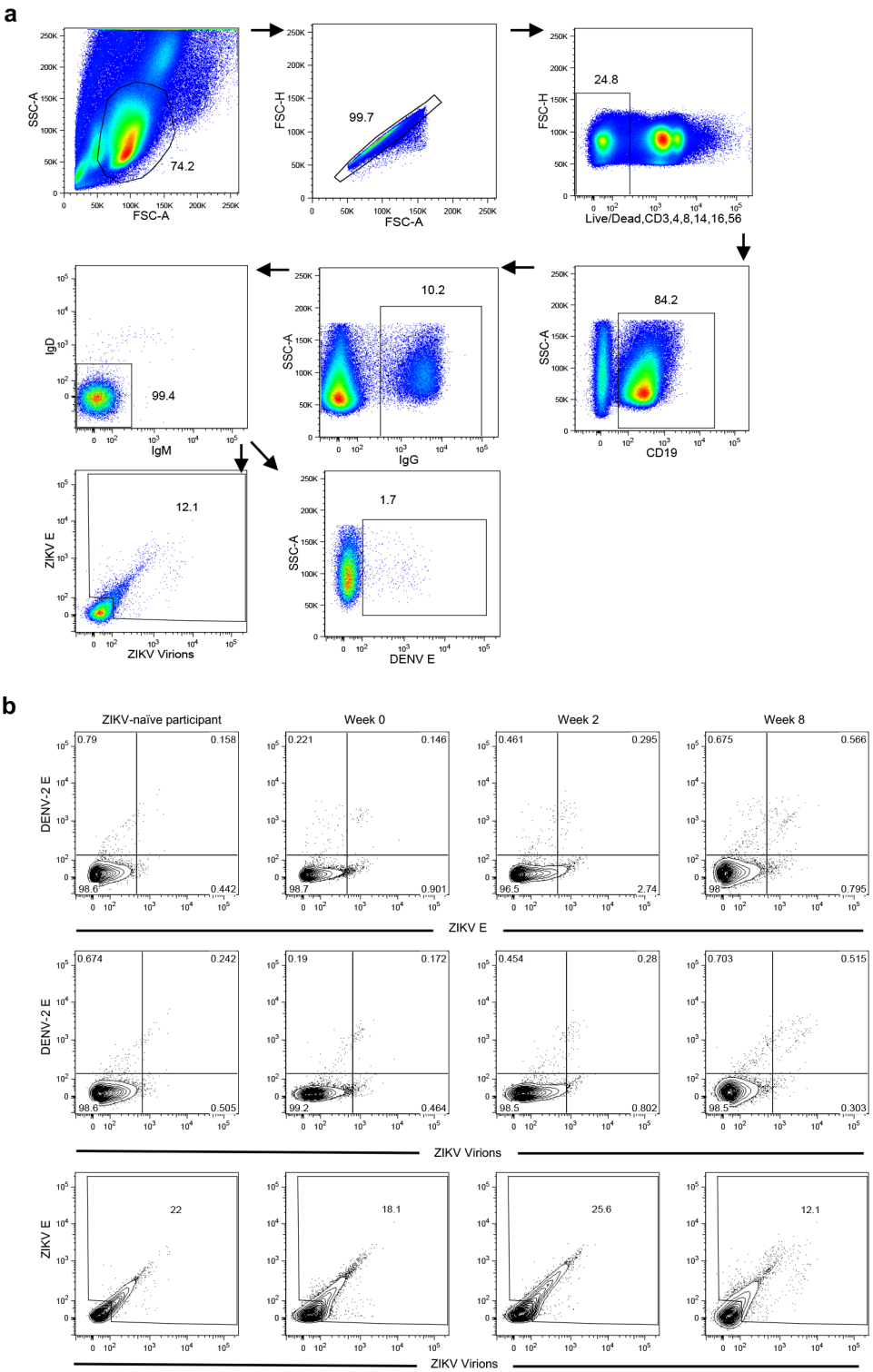

Extended Data Fig. 1 | Flow cytometry gating strategy. a, Gating strategy and flow cytometry plots of peripheral blood mononuclear cells from Participant A at week 8. $CD19^{+}IgG^{+}IgD^{-}IgM^{-}$ B cells reactive to whole ZIKV virions, ZIKV E, and DENV-2 E were sorted into lysis buffer for B cell Receptor (BCR) sequencing. **b**, Flow cytometry plots of antigen-positive B cells from a known ZIKV-naïve participant and week 0, week 2, and week 8 PBMCs from Participant A. PBMCs at week 8 were sorted on a different day compared to PBMCs from week 0 and week 2 and the ZIKV-naïve participant. Increased frequencies of antigen-specific and cross-reactive B cells were detected against all antigens (whole ZIKV virions, ZIKV E, and DENV-2 E) between week 0 and week 2 in Participant A. A single sort was performed for each time point.

		Binding (OD)		Neutralization (IC_{50}, ng ml^{-1})					
	mAb	ZIKV	DENV-2	ZIKV	DENV-1	DENV-2	DENV-3	DENV-4	
1	MHRP-Z1001	+++	+++	7.5	919.3	1.9	40.0	286.6	ZIKV/DENV cross neutralizing
2	MHRP-Z1004	+++	+++	1.0	263.0	1.8	16.5	238.9	
3	MHRP-Z1024	+++	+++	22.6	151.6	1.3	15.9	356.6	
4	MHRP-Z1020	+++	+++	161.1	28.9	18.9	65.1	14.9	
5	MHRP-Z1054	+++	+++	1,111.9	92.1	72.2	206.4	63.3	
6	MHRP-Z1056*	+++	+++	50,000	108.8	207.8	486.9	154.1	
7	MHRP-Z1118**	+++	++++	10,009.3	29.4	5.3	4.9	12,303.3	
8	MHRP-Z1098	+++	+++	50,000	80.0	116.9	1,490.4	6.8	DENV1-4 cross neutralizing
9	MHRP-Z1100	+++	+++	50,000	34.9	84.5	291.5	9.6	
10	MHRP-Z1073	+++	++++	50,000	64.3	70.1	408.7	9.8	
11	MHRP-Z1105	++++	++++	50,000	56.5	124.7	643.1	10.4	
12	MHRP-Z1109	++++	+++	50,000	99.2	113.2	365.7	11.1	
13	MHRP-Z1091	+++	+++	50,000	63.1	182.4	211.7	13.6	
14	MHRP-Z1069	+++	+++	50,000	214.6	134.4	3,232.6	23.2	
15	MHRP-Z1017	++++	++++	50,000	91.8	136.7	1,244.6	26.0	
16	MHRP-Z1072	++++	+++	50,000	35.4	116.0	461.8	26.2	
17	MHRP-Z1021	+++	+++	50,000	144.6	260.0	1,726.6	28.9	
18	MHRP-Z1114	+++	++++	50,000	143.2	235.6	1,562.8	29.2	
19	MHRP-Z1063	+++	+++	50,000	68.9	65.2	1,322.8	30.0	
20	MHRP-Z1083	+++	+++	50,000	51.7	158.2	2,364.1	31.1	
21	MHRP-Z1003	+++	+++	50,000	60.0	30.3	906.9	32.0	
22	MHRP-Z1111	++++	+++	50,000	142.0	306.7	1,271.3	34.2	
23	MHRP-Z1039	+++	+++	50,000	119.2	338.6	2,866.9	36.7	
24	MHRP-Z1012	+++	+++	50,000	34.5	92.0	437.0	38.6	
25	MHRP-Z1096	+++	++++	50,000	72.4	32.8	1,253.6	38.7	
26	MHRP-Z1055	+++	+++	50,000	72.1	78.9	806.2	40.0	
27	MHRP-Z1102	+++	+++	50,000	106.1	204.5	1,848.3	41.2	
28	MHRP-Z1090	+++	+++	50,000	54.4	92.2	3,154.3	42.7	
29	MHRP-Z1084	+++	++++	50,000	63.2	72.3	484.6	42.9	
30	MHRP-Z1077	+++	+++	50,000	28.2	116.7	384.5	45.2	
31	MHRP-Z1059	+++	+++	50,000	170.5	99.7	3,269.4	47.8	
32	MHRP-Z1115	+++	+++	50,000	134.4	277.2	1,209.8	51.0	
33	MHRP-Z1068	+++	++++	50,000	104.3	222.2	2,914.2	54.8	
34	MHRP-Z1101	+++	+++	50,000	85.4	39.7	648.0	54.9	
35	MHRP-Z1060	+++	+++	50,000	93.8	152.6	1,245.2	59.6	
36	MHRP-Z1015	+++	+++	50,000	314.6	183.4	2,322.9	68.0	
37	MHRP-Z1002	+++	+++	50,000	187.7	270.3	1,943.3	69.6	
38	MHRP-Z1074	++	+++	50,000	865.3	147.3	9,833.7	71.8	
39	MHRP-Z1080	+++	+++	50,000	104.0	199.9	1,886.9	84.4	
40	MHRP-Z1041	+++	++	50,000	313.5	588.7	5,256.2	155.3	
41	MHRP-Z1035	+++	+++	50,000	847.4	547.4	10,150.2	157.5	
42	MHRP-Z1117	+++	+++	50,000	526.6	575.5	2,900.1	245.0	
43	MHRP-Z1089	+++	+++	50,000	228.8	542.1	1,827.9	254.7	
44	MHRP-Z1110	+++	+++	50,000	2,048.3	326.8	2,033.0	278.7	
45	MHRP-Z1038	+++	+++	50,000	159.9	155.5	1,829.5	310.8	
46	MHRP-Z1062	++++	+++	50,000	35.4	220.6	6,362.0	50,000	Any DENV neutralizing
47	MHRP-Z1104	++	+++	50,000	50,000	4.0	50,000	10.2	
48	MHRP-Z1043	++	+++	50,000	5,991.5	50,000	50,000	11,356.7	
49	MHRP-Z1037	-	+++	50,000	50,000	2.1	50,000	50,000	
50	MHRP-Z1048	+	+++	50,000	50,000	6.1	50,000	50,000	
51	MHRP-Z1051	-	+++	50,000	50,000	18.5	50,000	50,000	
52	MHRP-Z1058	-	+++	50,000	50,000	23.6	50,000	50,000	
53	MHRP-Z1057	++	+++	50,000	50,000	1,701.3	50,000	50,000	
54	MHRP-Z1078	+++	++++	50,000	50,000	50,000	50,000	17,751.5	
55	MHRP-Z1013	+++	+++	50,000	50,000	50,000	50,000	50,000	Non-neutralizers
56	MHRP-Z1088	+++	++	50,000	50,000	50,000	50,000	50,000	
57	MHRP-Z1022	+++	-	50,000	50,000	50,000	50,000	50,000	
58	MHRP-Z1057	++	+++	50,000	50,000	50,000	50,000	50,000	
59	MHRP-Z1031	++	++	50,000	50,000	50,000	50,000	50,000	
60	MHRP-Z1075	++	+	50,000	50,000	50,000	50,000	50,000	
61	MHRP-Z1052	++	-	50,000	50,000	50,000	50,000	50,000	
62	MHRP-Z1009	+	++	50,000	50,000	50,000	50,000	50,000	
63	MHRP-Z1018	+	++	50,000	50,000	50,000	50,000	50,000	
64	MHRP-Z1034	+	++	50,000	50,000	50,000	50,000	50,000	
65	MHRP-Z1108	+	++	50,000	50,000	50,000	50,000	50,000	
66	MHRP-Z1007	+	+	50,000	50,000	50,000	50,000	50,000	
67	MHRP-Z1023	+	+	50,000	50,000	50,000	50,000	50,000	
68	MHRP-Z1028	+	+	50,000	50,000	50,000	50,000	50,000	
69	MHRP-Z1030	+	+	50,000	50,000	50,000	50,000	50,000	
70	MHRP-Z1032	+	+	50,000	50,000	50,000	50,000	50,000	
71	MHRP-Z1042	+	+	50,000	50,000	50,000	50,000	50,000	
72	MHRP-Z1053	+	+	50,000	50,000	50,000	50,000	50,000	
73	MHRP-Z1067	+	+	50,000	50,000	50,000	50,000	50,000	
74	MHRP-Z1076	+	+	50,000	50,000	50,000	50,000	50,000	
75	MHRP-Z1106	+	+	50,000	50,000	50,000	50,000	50,000	
76	MHRP-Z1112	+	+	50,000	50,000	50,000	50,000	50,000	
77	MHRP-Z1006	+	-	50,000	50,000	50,000	50,000	50,000	
78	MHRP-Z1027	+	-	50,000	50,000	50,000	50,000	50,000	
79	MHRP-Z1086	+	-	50,000	50,000	50,000	50,000	50,000	
80	MHRP-Z1061	-	+++	50,000	50,000	50,000	50,000	50,000	
81	MHRP-Z1000	-	++	50,000	50,000	50,000	50,000	50,000	
82	MHRP-Z1071	-	++	50,000	50,000	50,000	50,000	50,000	
83	MHRP-Z1119	-	++	50,000	50,000	50,000	50,000	50,000	

*: Z1056 neutralized ZIKV in the FlowNT assay with an IC_{50} of 235.8 ng ml^{-1}
**: Z1118 did not neutralize ZIKV in the FlowNT assay

Extended Data Fig. 2 | Cross-neutralization characteristics of isolated antibodies. Heat map of binding (shades of blue) and neutralization (shades of red) titrations of all antibodies isolated from Participant A that bound to ZIKV and/or DENV-2 virions. Binding data are reported as follows: - (below background), + (OD<0.5), ++ (OD 0.5-1.0), +++ (OD 1.0-1.5) and ++++ (OD>1.5). Shown are geometric mean neutralizing titers of ZIKV and DENV1-4 from at least 2 independent experiments with the IC_{50} values indicated (ng ml^{-1}).

a

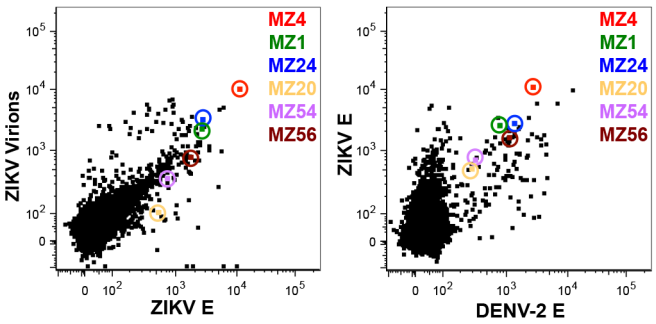

b

	ZIKV	DENV-1	DENV-2	DENV-3	DENV-4	JEV, WNV, YFV	IC_{50} (ng ml^{-1})
MZ1	7.5	919.3	1.9	40.0	286.6	>50,000	<5
MZ4	1.0	263.0	1.8	16.5	238.9	>50,000	5-50
MZ24	22.6	151.6	1.3	15.9	356.6	>50,000	50-500
EDE1-C8	104.3	23.4	50.0	51.8	146.6	>50,000	500-5,000
EDE2-A11	511.7	9.9	14.7	8.5	6.5	>50,000	>5,000
Z004	1.4	1.8	>50,000	>50,000	>50,000	>50,000	>50,000

c d e

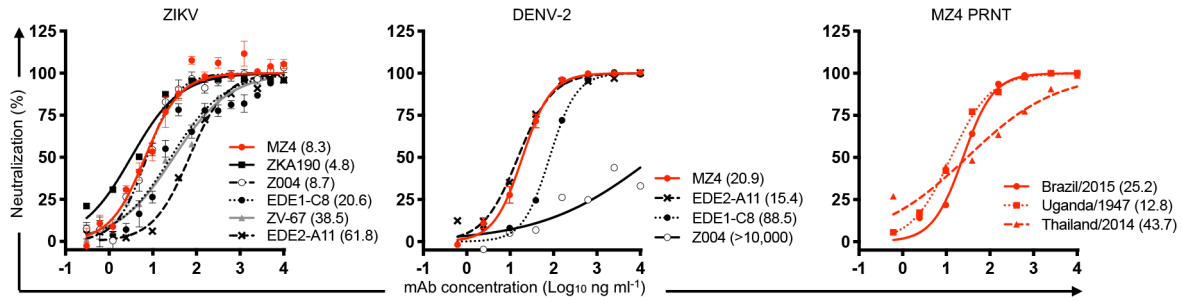

Extended Data Fig. 3 | Antibody isolation and neutralizing characteristics of MZ4 family antibodies. a, Isolation of whole ZIKV virion, ZIKV E and DENV-2 E reactive $CD19^+/IgG^+$ B cells 4 weeks following the second ZPIV immunization (week 8) from Participant A. Individual B cells encoding ZIKV-neutralizing mAbs are indicated in the flow cytometry plots. **b**, Neutralization heat map of the MZ4 family and control mAbs against ZIKV PR, DENV1-4, JEV, WNV and YFV, with the microneutralization IC_{50} values indicated (ng ml^{-1}). **c**,**d**, FlowNT neutralization of MZ4 against (c) ZIKV (Paraiba_01) and (d) DENV-2 (S16803) compared to other potent ZIKV/DENV cross-neutralizing and specific antibodies. All mAbs were tested in at least 2 independent experiments. Where shown, error bars indicate mean ± s.e.m. for mAbs tested in 3 independent experiments. **e**, PRNT neutralization of MZ4 against ZIKV strains of American, Asian and African lineages, indicated by country of origin and date of isolation. Shown is the mean % neutralization from a single experiment using triplicates. The IC_{50} neutralization titers (ng ml^{-1}) are indicated in parentheses for each mAb.

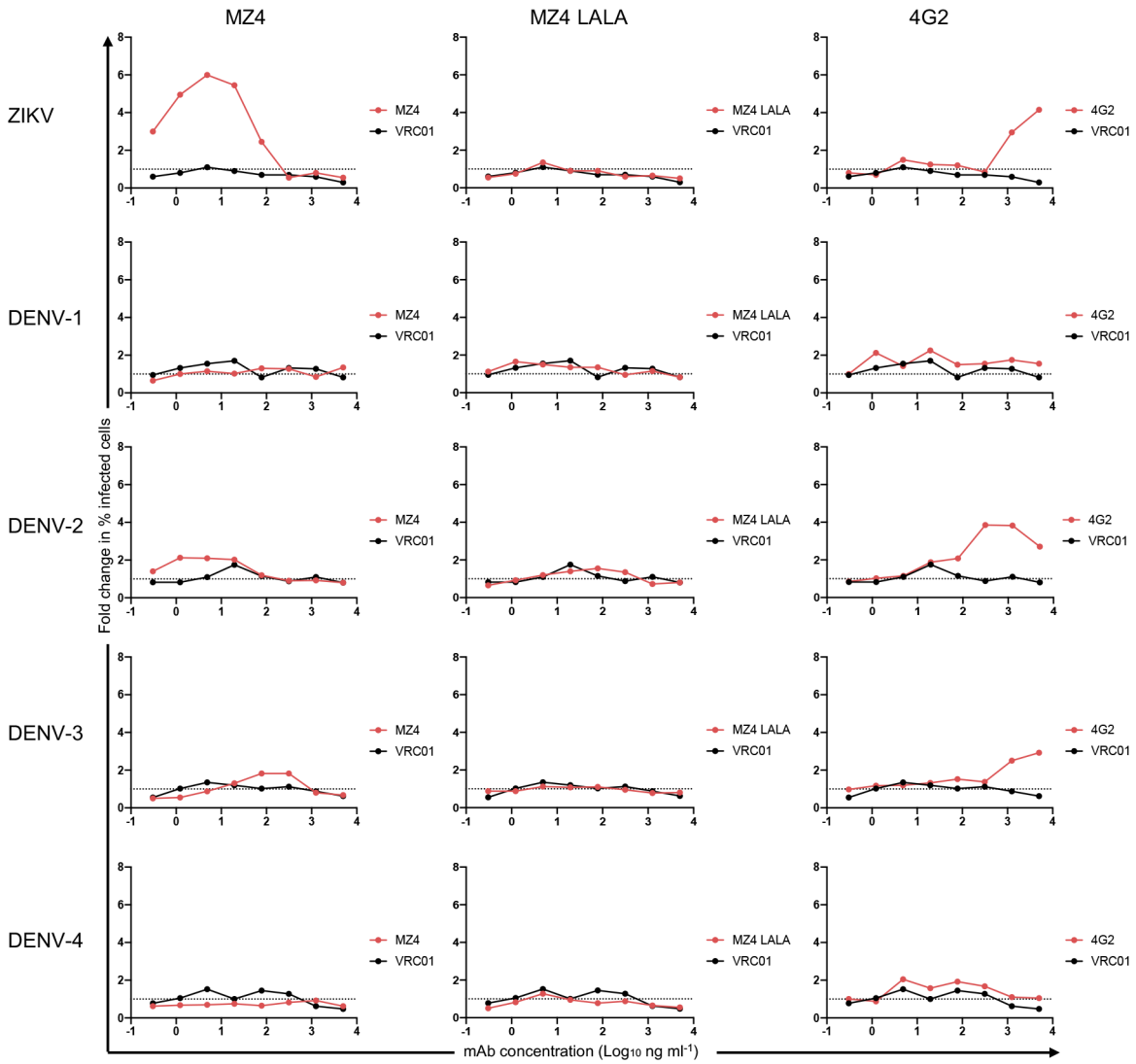

Extended Data Fig. 4 | *In vitro* antibody dependent enhancement (ADE). MZ4, MZ4 harboring the Fc mutations abolishing binding to Fcγ receptors (MZ4 LALA) and the pan flavivirus FLE antibody 4G2 were tested in a flow cytometry-based assay for their ability to enhance infection in K562 cells. ADE is reported as fold change in percent of infected cells relative to baseline percent infection of K562 cells (in absence of antibody, dotted line). The HIV-1 specific antibody VRC01 served as negative control. Shown is the mean from 2 independent experiments performed in duplicates.

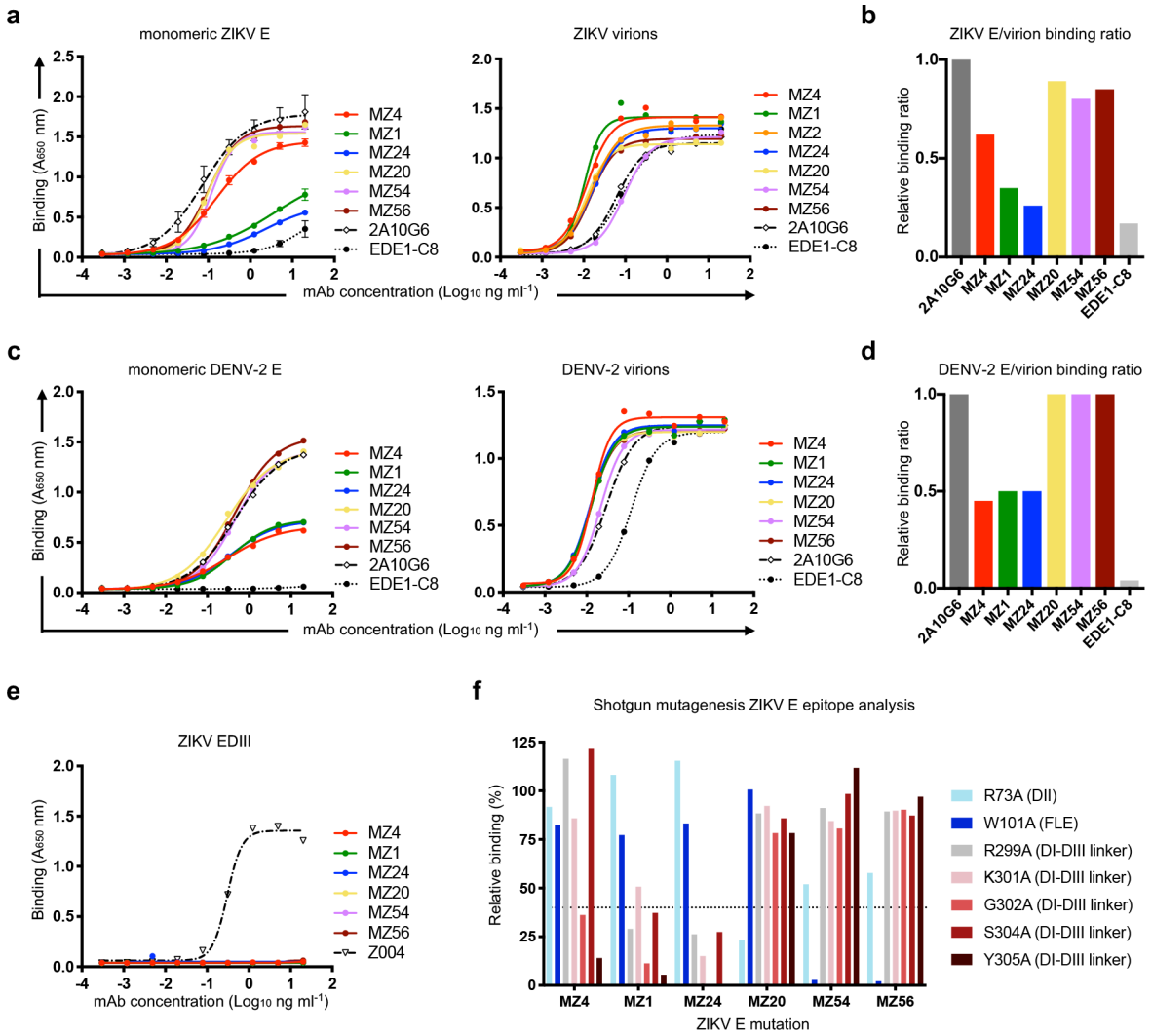

Extended Data Fig. 5 | Antibody binding characteristics and epitope mapping. a-**d**, Binding of ZIKV-neutralizing mAbs to ZIKV and DENV-2 monomeric E proteins, and whole ZIKV and DENV-2 virions by ELISA. **a**, Binding to monomeric ZIKV E (left) and virions (right). Shown is the mean from 3 (± s.e.m as indicated by error bars) or 2 independent experiments. **b**, Relative binding ratio of monomeric ZIKV E to ZIKV whole virions calculated from (a). Antibodies with low ratio values were characteristic of quaternary epitopes, such as EDE1-C8, whereas ratios closer to 1 were characteristic of monomeric recognition similar to an FLE antibody, such as 2A10G6, which binds to both monomeric E and ZIKV. **c**, Binding to monomeric DENV-2 E (left) and whole DENV-2 virions (right). Shown is the mean of 2 independent experiments. **d**, Relative binding ratio of monomeric DENV-2 E to DENV-2 whole virions calculated from (c). **e**, Binding of mAbs to ZIKV E recombinant DIII domain assessed by ELISA. Shown is the mean of 2 independent experiments. **f**, Shotgun mutagenesis ZIKV E epitope analysis. Relative binding to ZIKV prM/E for individual mutations is plotted. Residues from which substitution to alanine causes >60% loss in binding (dotted line) were considered important for binding. Shown is the mean of duplicates from a single experiment.

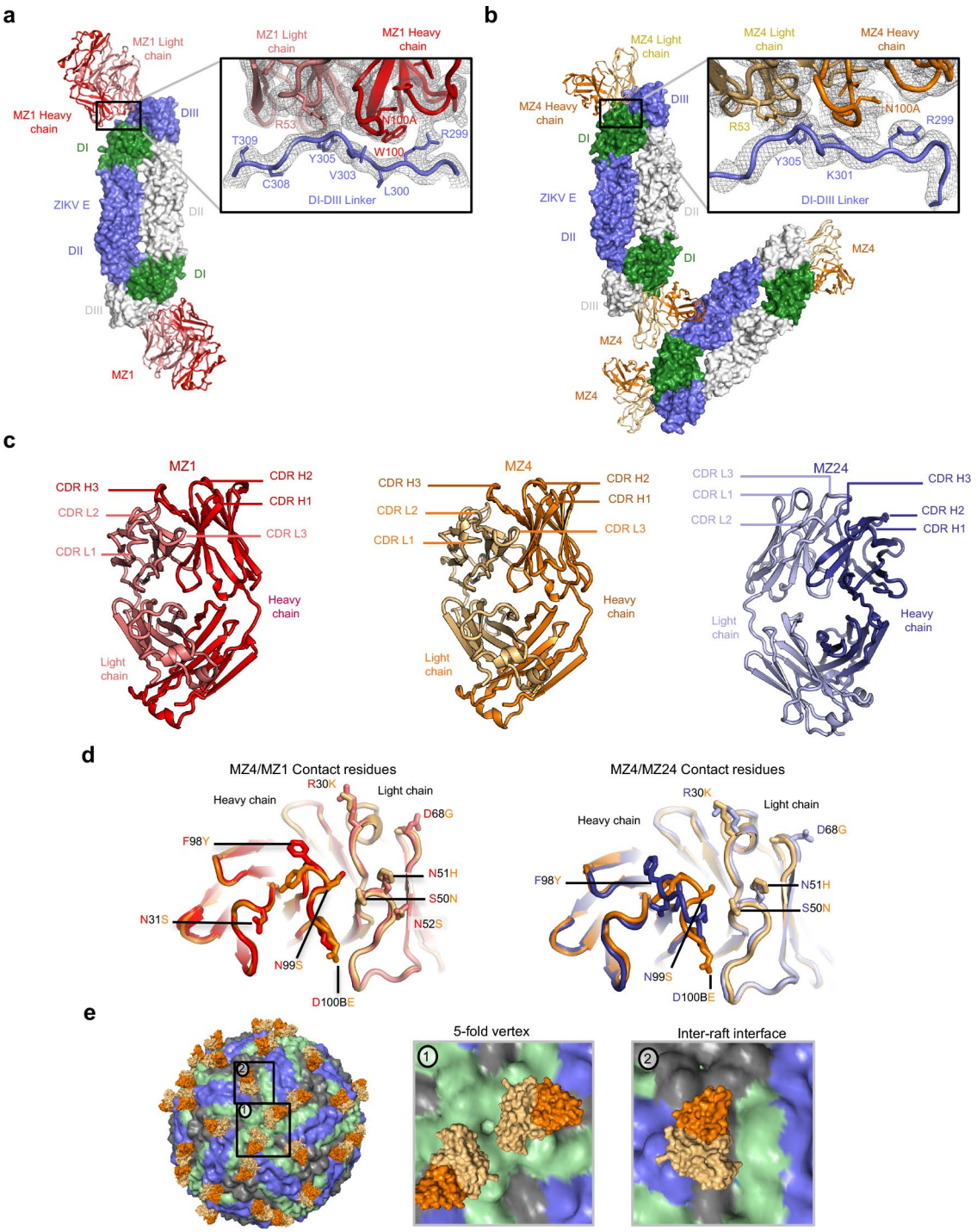

Extended Data Fig. 6 | Structural analysis of MZ4 family antibodies. a, MZ1-ZIKV E crystal structure asymmetric unit contents. ZIKV E is shown in surface representation (DII and DIII [blue] and DI [dark green]), and MZ1 Fab is shown in ribbon representation (heavy chain [red] and light chain [salmon]). Zoom-in window shows the $2F_o$-F_c electron density for the MZ1-DI/DIII linker interaction (gray mesh representation contoured at 1.5σ). **b**, MZ4-ZIKV E crystal structure asymmetric unit contents. Four MZ4 Fv molecules bound to four molecules of ZIKV E were observed in the asymmetric unit. ZIKV E protomers within a dimer are shown in surface representation (blue and white with DI dark green). MZ4 antibody heavy and light chains are shown in ribbon representation (dark and light orange). Zoom-in window shows the $2F_o$-F_c electron density for the MZ4-DI/DIII linker interaction (gray mesh contoured at 1.0σ). **c**, Crystal structure of MZ1, MZ4, and MZ24 Fab molecules are shown in ribbon representation with light and heavy chain CDRs indicated. **d**, Overlay of MZ1 and MZ4 (left), and MZ4 and MZ24 (right) Fab structures. Antigen-contacting residues that differ between MZ4 and the other family members are shown in stick representation and amino acid changes are indicated. **e**, Model of MZ4 Fv on the ZIKV (PDB: 5IRE). MZ4 is shown in surface representation (dark [heavy chain] and light [light chain] orange). E protomers on the ZIKV virion are colored blue, gray, and green, which indicates dimeric, trimeric, and pentameric vertex interfaces, respectively. Close-up view of the modelled MZ4 interactions at the five-fold vertex (1) and inter-raft interface (2) are shown.

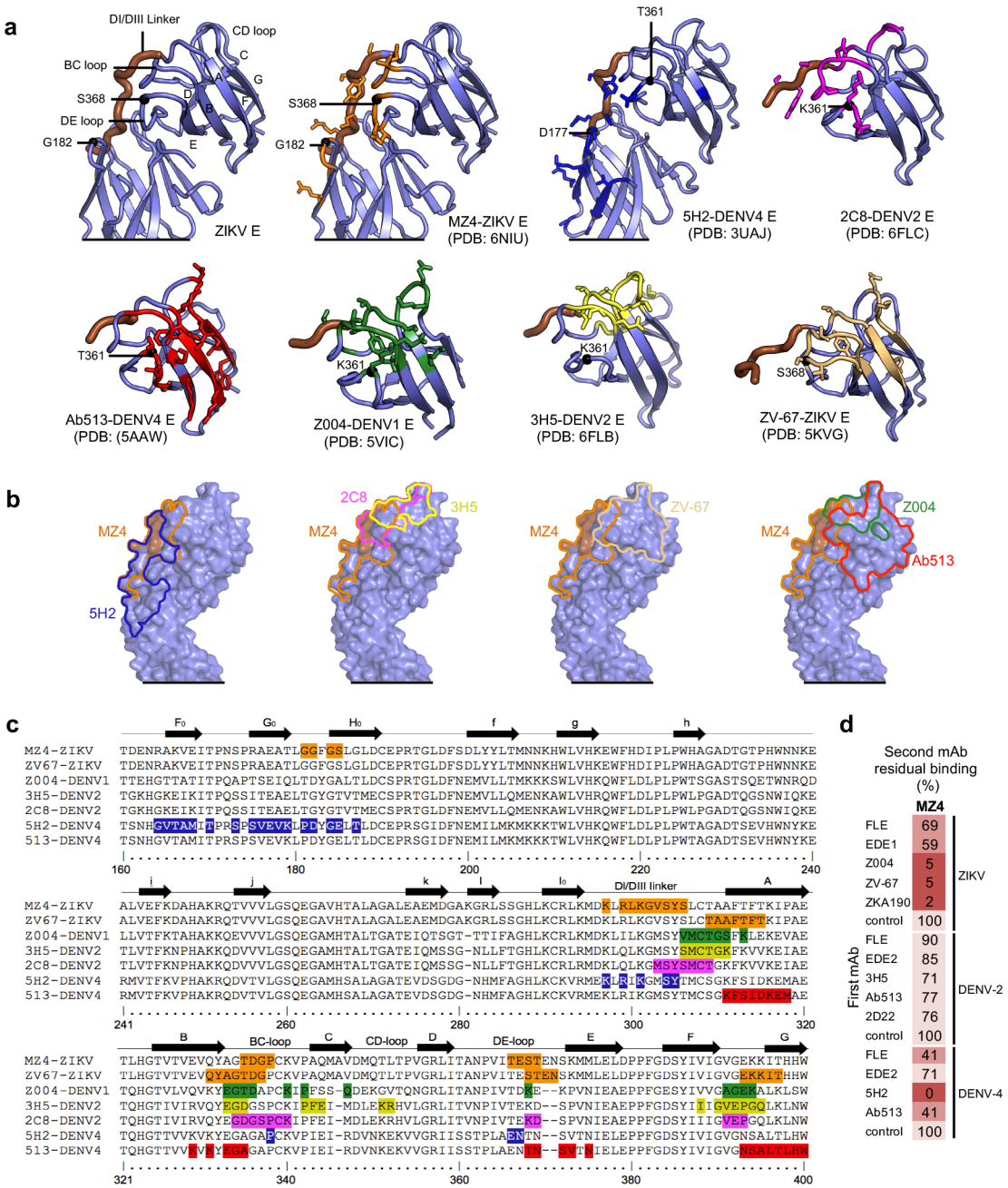

Extended Data Fig. 7 | Epitope recognition by antibody MZ4. a, Flavivirus-neutralizing antibodies that recognize DIII and adjacent regions. Flavivirus E molecules are shown in ribbon representation with the DIII, DI/DIII linker region, and lateral ridge loop architecture shown on the top left for reference. Antibody contact residues (defined using PISA) are shown in stick representation and colored as follows: MZ4 (orange), 5H2 (dark blue), 2C8 (magenta), Ab513 (red), Z004 (green), 3H5 (yellow), and ZV-67 (light orange). ZIKV E – MZ4 contact residues G182 and S368 (and DENV equivalent residues), are shown as black spheres. **b**, Antibody epitopes are indicated as colored solid lines on the surface of ZIKV E (blue, with the DI/DIII linker in brown). **c**, Sequence alignment of flavivirus E proteins (residues 160-400, ZIKV numbering). Antibody contact residues on flavivirus E proteins are highlighted. **d**, MZ4 antibody binding competitions. Competition between the indicated first mAb and MZ4 for binding to the relevant E protein were performed as described in Fig. 1h. Shading from dark to light red indicates competition strength ranging from strong (0-30%), to intermediate (31-69%), to weak/none (70-100%).

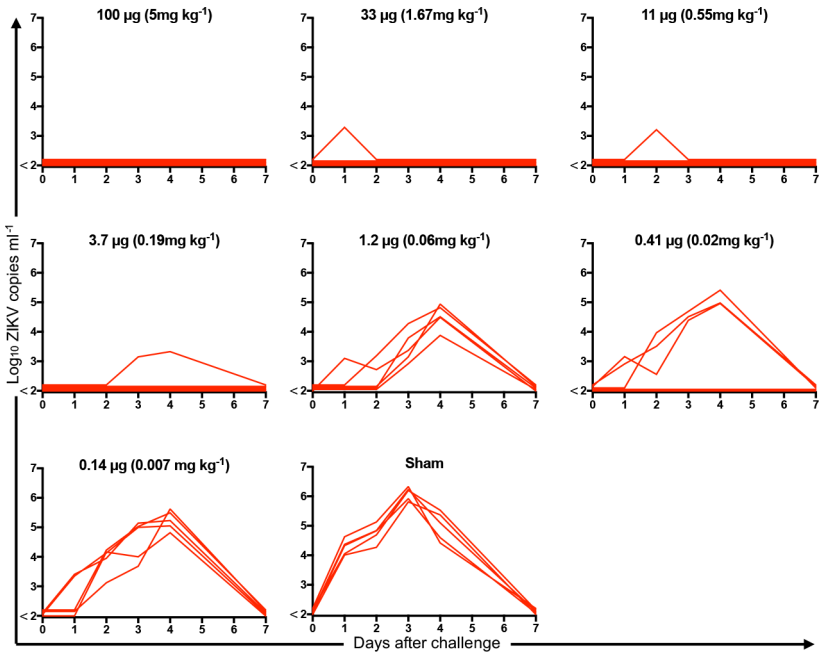

Extended Data Fig. 8 | *In vivo* titration of MZ4 prophylactic dose. Forty naïve Balb/c mice were infused intravenously with the indicated dose (n=5/dose) of MZ4 or saline (sham). Two hours later, mice were challenged with 10^5 viral particles (10^2 plaque-forming units) of ZIKV BR/2015 intravenously. Following infusion with the indicated dose or saline (sham), ZIKV viral loads were measured post-challenge by RT–PCR.

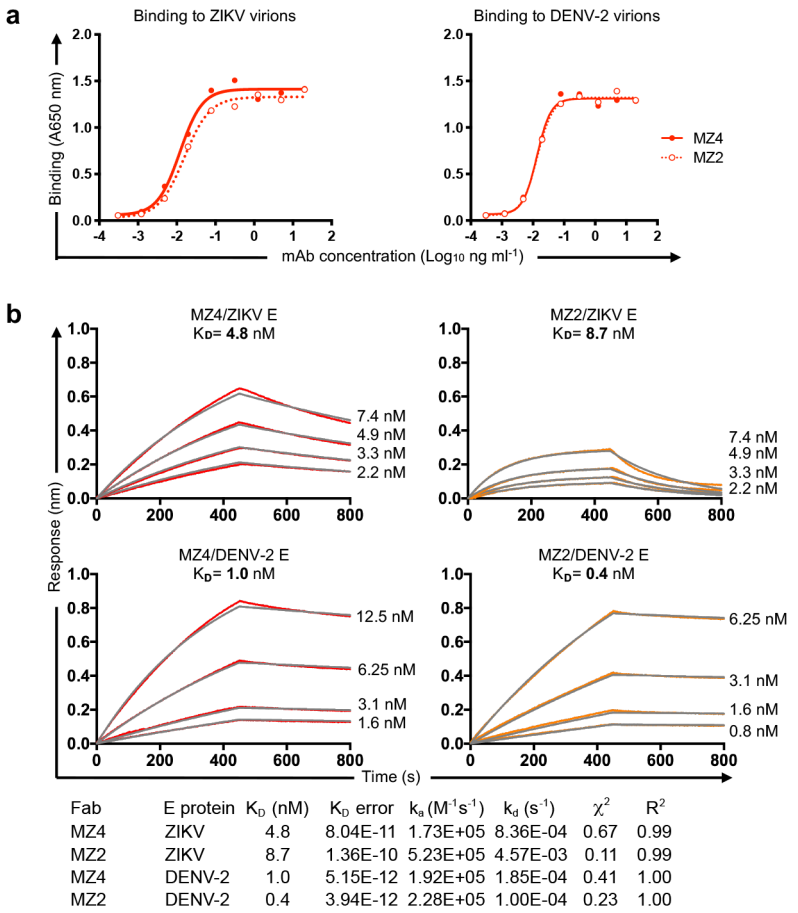

Fab	E protein	K_D (nM)	K_D error	k_a ($M^{-1}s^{-1}$)	k_d (s^{-1})	χ^2	R^2
MZ4	ZIKV	4.8	8.04E-11	1.73E+05	8.36E-04	0.67	0.99
MZ2	ZIKV	8.7	1.36E-10	5.23E+05	4.57E-03	0.11	0.99
MZ4	DENV-2	1.0	5.15E-12	1.92E+05	1.85E-04	0.41	1.00
MZ2	DENV-2	0.4	3.94E-12	2.28E+05	1.00E-04	0.23	1.00

c

	MZ4	MZ2	IC_{50} (ng ml^{-1})
ZIKV	1.0	2.7	<5
DENV-1	263.0	486.2	5-50
DENV-2	1.8	2.6	50-500
DENV-3	16.5	15.9	500-5,000
DENV-4	238.9	420.4	>5,000
JEV, WNV, YFV	>50,000	>50,000	>50,000

d

ZIKV/ DENV-2 E residue	MZ2	MZ4
R299/Q293	✔	✔
L300/L294		✔
K301/K295	✔	✔
G302/G296	✔✔	✔✔
Y305/Y299	✔✔	✔✔

ZIKV 297 299 302 305 308 KLRLKGVSYSLC
DENV-2 291 293 294 295 296 299 302 KLQLKGMSYSMC

Extended Data Fig. 9 | Characteristics of MZ2, isolated two weeks after the first ZPIV vaccination. a, Binding of MZ4 and MZ2 to ZIKV (left) and DENV-2 (right) virions, assessed by ELISA. Shown is the mean from 2 independent experiments. **b**, Binding kinetics of MZ4 and MZ2 antibodies to ZIKV (top) and DENV-2 (bottom) E proteins as measured by BLI. Affinity constants (K_D) were calculated from binding curves (red [MZ4] and orange [MZ2] obtained from 4 serial dilutions of Fabs and fitted (grey curves) from a single experiment using a 1:1 binding model. Below, summary table of binding kinetic constants and fit parameters. **c**, Microneutralization heat map of MZ4 and MZ2 against ZIKV, DENV1-4, JEV, WNV and YFV, with the IC_{50} values indicated (ng ml^{-1}). **d**, Shotgun mutagenesis ZIKV and DENV-2 E epitope analysis. Residues critical for binding are indicated by check marks. Below, alignment of ZIKV and DENV-2 DI/DIII linkers with respective residue numbering.

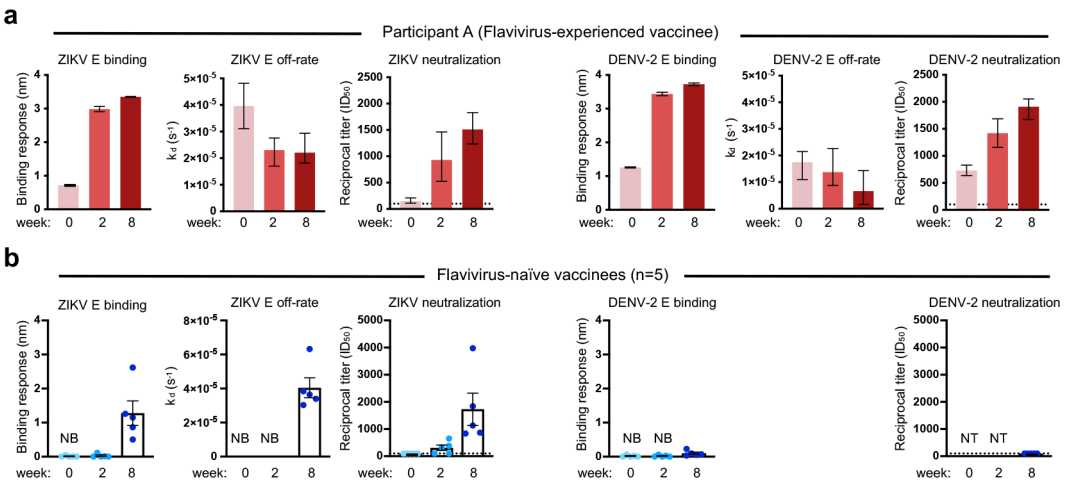

Extended Data Fig. 10 | Additional characterization of polyclonal antibody responses in flavivirus-experienced and flavivirus-naïve vaccinated participants. a, **b**, Polyclonal antibody binding, off-rates and neutralization titers (FlowNT) to ZIKV (left) or DENV-2 (right) of (**a**, red) Participant A (n=1) and (**b**, blue) flavivirus-naïve vaccinees (5 donors with the highest responses) at baseline (week 0), 2 weeks following the first vaccination (week 2) and 4 weeks following the second vaccination (week 8). For (a), shown is the mean titer or off-rate and range from at least 2 independent experiments. For (b), shown is the mean titer per individual with s.e.m. indicated by the error bars per assay. Plasma binding responses and affinity off-rates to the indicated E protein (nm) were measured by BLI; NB=no binding detected. Plasma dilution series were used to calculate off-rates or dissociation constants (k_d, s^{-1}) against the indicated E protein. Lower off-rates indicate slower dissociation and higher affinity. Dotted line indicates lower limit of detection. As no DENV-2 neutralization was observed for naïve donors at week 8, week 0 and 2 were not tested (NT).

nature research

Corresponding author(s): Shelly J. Krebs (skrebs@hivresearch.org) and M. Gordon Joyce (gjoyce@hivresearch.org)

Last updated by author(s): Dec 3, 2019

Reporting Summary

Nature Research wishes to improve the reproducibility of the work that we publish. This form provides structure for consistency and transparency in reporting. For further information on Nature Research policies, see Authors & Referees and the Editorial Policy Checklist.

Statistics

For all statistical analyses, confirm that the following items are present in the figure legend, table legend, main text, or Methods section.

n/a	Confirmed	
☐	☒	The exact sample size (*n*) for each experimental group/condition, given as a discrete number and unit of measurement
☐	☒	A statement on whether measurements were taken from distinct samples or whether the same sample was measured repeatedly
☐	☒	The statistical test(s) used AND whether they are one- or two-sided *Only common tests should be described solely by name; describe more complex techniques in the Methods section.*
☐	☒	A description of all covariates tested
☒	☐	A description of any assumptions or corrections, such as tests of normality and adjustment for multiple comparisons
☐	☒	A full description of the statistical parameters including central tendency (e.g. means) or other basic estimates (e.g. regression coefficient) AND variation (e.g. standard deviation) or associated estimates of uncertainty (e.g. confidence intervals)
☐	☒	For null hypothesis testing, the test statistic (e.g. *F*, *t*, *r*) with confidence intervals, effect sizes, degrees of freedom and *P* value noted *Give P values as exact values whenever suitable.*
☒	☐	For Bayesian analysis, information on the choice of priors and Markov chain Monte Carlo settings
☒	☐	For hierarchical and complex designs, identification of the appropriate level for tests and full reporting of outcomes
☒	☐	Estimates of effect sizes (e.g. Cohen's *d*, Pearson's *r*), indicating how they were calculated

Our web collection on statistics for biologists contains articles on many of the points above.

Software and code

Policy information about availability of computer code

Data collection	Diffraction data were collected at Advanced Photon Source (APS), Argonne National Laboratory beamlines, and at National Synchrotron Light Source II (NSLS-II). Diffraction data for MZ1 Fab, and MZ4 Fab were collected at APS 19-ID beamline to a final resolution of 2.05Å, and 2.95Å, respectively, using a Q315r CCD detector. Diffraction data for MZ1-ZIKV E crystals were collected at APS 24-ID-E beamline, and measured using a Dectris Eiger 16M PIXEL detector to a final resolution of 4.2 Å. Diffraction data for MZ4-ZIKV E complex were collected at APS 19-BM beamline, and measured using an ADSC Quantum 210r CCD detector to a final resolution of 4.3 Å. MZ24 Fab diffraction data were collected at beamline NSLS-II AMX 17-ID-1 and measured using a Eiger 9M PIXEL detector to a final resolution of 2.11 Å.
Data analysis	Statistical analyses were performed in Prism (version 8, GraphPad Software), N-Parameter Logistic Regression (nplr) R package version 0.1-7, R (version 3.5.1) and R studio (1.1.442). Data were graphed using Prism software (version 7, GraphPad Software). Flow plots were generated using FlowJo version 9.9.6. Real-time interactions between purified E proteins and antibodies were measured by Biolayer interferometry and analyzed by the FortéBio Data Analysis software 9.0. Structural diffraction data indexing, integration, and scaling were carried out using the HKL2000 suite37. Phenix xtriage (version 1.11.1-2575-0000) was used to analyze all the scaled diffraction data output from HKL2000 (suite 37) and XDS (version Jan 26, 2018 BUILT=20180126), and structure quality was assessed with MolProbity (Phenix suite version 1.11.1-2575-0000). All crystal structures described in this study were solved by molecular replacement using the program Phaser, version 2.139. All structure figures were generated using PyMOL (version 1.3). MZ1-ZIKV E and MZ4-ZIKV E contact residues and previously described flavivirus-neutralizing antibody-E contact residues were identified using PISA (PDBePISA v1.52 [20/10/2014]).

For manuscripts utilizing custom algorithms or software that are central to the research but not yet described in published literature, software must be made available to editors/reviewers. We strongly encourage code deposition in a community repository (e.g. GitHub). See the Nature Research guidelines for submitting code & software for further information.

Data

Policy information about availability of data

All manuscripts must include a data availability statement. This statement should provide the following information, where applicable:

- Accession codes, unique identifiers, or web links for publicly available datasets
- A list of figures that have associated raw data
- A description of any restrictions on data availability

The associated accession numbers for the coordinates and structure factors reported in this paper are Protein Data Bank ID: 6MTX, 6MTY, 6NIP, 6NIU and 6NIS. The sequences for MZ4, MZ1, MZ2, MZ20, MZ24, MZ54, MZ56 heavy chains and MZ4, MZ1, MZ2, MZ20, MZ24, MZ54, MZ56 light chains have been deposited in GenBank under ID codes MN523667-MN523680, respectively. The data that support the findings of this study are available from the corresponding authors upon request. The interim aggregate data of ZPIV trial in Puerto Rico (NCT03008122) are available with permission from Division of Microbiology and Infectious Disease, NIAID, NIH, as this is currently an active, ongoing Phase I study.

Field-specific reporting

Please select the one below that is the best fit for your research. If you are not sure, read the appropriate sections before making your selection.

☒ Life sciences ☐ Behavioural & social sciences ☐ Ecological, evolutionary & environmental sciences

For a reference copy of the document with all sections, see nature.com/documents/nr-reporting-summary-flat.pdf

Life sciences study design

All studies must disclose on these points even when the disclosure is negative.

Sample size	Monoclonal antibodies were isolated from 1 individual (Participant A), who had the highest ZIKV neutralization titer within the vaccine clinical trial. Upon further analysis, this individual had prior flavivirus exposure. The responses from this individual were compared to the remaining vaccinated individuals within the Phase I trial who were flavivirus naive (N=24), with 5 individuals tested for additional cross-flavivirus neutralization. To determine if these observations were unique to Participant A, the kinetics and magnitude of ZIKV neutralization were compared to flavivirus-experienced individuals (N=34) from Puerto Rico who received the same ZPIV vaccination regimen, 5 of which were further tested for cross-neutralizing response to 7 other flaviviruses (DENV 1-4, WNV, JEV, and YFV). Passive transfer studies of monoclonal antibodies in mice were used to assess protection from in vivo DENV-2 and ZIKV viral replication using two different mouse models. To evaluate the efficacy of the monoclonal antibodies MZ2 and MZ4 against DENV-2 in the Ifnar-/- C57BL/6 weight loss model, three groups of 10 mice each received treatment with 200µg of MZ2, MZ4 or vehicle control prior to virus exposure. In vivo passive protection experiments using MZ4 were performed 3 separate occasions with ZIKV challenge using six to eight-week-old female Balb/c mice (n=5/group/occasion). Mice received 100 µl (200 µg) of a 2 mg ml-1 solution of purified monoclonal antibody prior to ZIKV exposure. To get an idea of the in vivo potency, 30 mice were used in a passive protection experiment with decreasing doses of MZ4 using a 3-fold dilution starting at 100µg (5mg kg-1) to 0.14µg (0.07 mg kg-1).
Data exclusions	No data were excluded from this analysis.
Replication	Binding and neutralization data were calculated from two independent experiments, performed in triplicate. Since there is inherent variability in different neutralization assays, 3 different types of neutralization assays (MN50, PRNT, and FlowNT5) were performed to confirm the observations. Neutralization potencies obtained from each assay correlated for all mAbs tested, and all findings were replicated. The passive protection experiments were performed 3 times with 5 mice each with MZ4 using a dose of 200µg (10 mg kg-1), which yielded 100% protection in all experiments.
Randomization	Flavivirus-naive status at baseline (as determined by neutralization against ZIKV, DENV 1-4, YFV, WNV, and JEV) was a prerequisite for enrolling in the Phase 1 WRAIR ZPIV vaccination trial. Prior flavivirus-exposure at baseline was not a prerequisite to enroll in the Puerto Rico ZPIV vaccine clinical trial. Randomization within each trial was not performed. For the in vivo mouse passive protection studies, Ifnar-/- C57BL/6 mice or female Balb/c mice were randomly assigned either treatment or sham groups, respectively, for each study.
Blinding	The Principal Investigators of the Phase I Clinical Trial as well as all other investigators were blinded during each of the trials. Samples from Participant A were chosen for monoclonal antibody isolation based upon high neutralization at peak timepoints and compared to the study participants enrolled in other trials using the same vaccination regimen. Investigators are currently still blinded for the ZPIV Phase I trial in Puerto Rico, study NCT03008122. The subset of of 5 individuals for cross-neutralization experiments was randomly selected by a contracted organization who oversees the clinical data collection while keeping the investigators and sponsor blinded. These 5 individuals were randomly selected based upon flavivirus exposure prior to ZPIV vaccination as determined by microneutralization. The Principle Investigators were also blinded to the treatment and sham groups for the in vivo mouse passive protection studies until the studies were complete and results were available.

Reporting for specific materials, systems and methods

We require information from authors about some types of materials, experimental systems and methods used in many studies. Here, indicate whether each material, system or method listed is relevant to your study. If you are not sure if a list item applies to your research, read the appropriate section before selecting a response.

Materials & experimental systems

n/a	Involved in the study
☐	☒ Antibodies
☐	☒ Eukaryotic cell lines
☒	☐ Palaeontology
☐	☒ Animals and other organisms
☐	☒ Human research participants
☐	☒ Clinical data

Methods

n/a	Involved in the study
☒	☐ ChIP-seq
☐	☒ Flow cytometry
☒	☐ MRI-based neuroimaging

Antibodies

Antibodies used

Antibodies not described in this study for the first time and their sources are as follows: Human recombinant EDE1-C8 (Barba-Spaeth et al., 2016), Human recombinant Z004 (Robbiani et al., 2017), Human recombinant Z3L1 (Wang et al., 2016), Human recombinant VRC01 (Wu et al., 2010), Mouse recombinant 2A10G6 (Deng et al., 2011), Mouse anti-pan-flavivirus E 6B6-C1 (J.T. Roehrig, CDC, Catalog PUR001, Lot A7031794), Mouse anti-pan-flavivirus E D1-4G2-4-15 (4G2) (Biovest/NCCC, Produced from ATCC Hybridoma D1-4G2-4-15 (ATCC® HB-112™), Lot 072110, Flow cytometry dilution 1/20), Mouse anti-monkey IgG, HRP conjugated (Southern Biotech, Catalog 4700-05, Lot A3814-M656D, Clone SB108a, Dilution 1/6000), Mouse anti-human IgG, HRP conjugated (Southern Biotech, Catalog 9040-05, Lot J3314.T085 and L0717-ZC27B, Clone JDC-10, Dilution 1/2800), Goat anti-mouse IgG, HRP conjugated (Southern Biotech, Catalog 1030-05, Lot K3515-T566E, Dilution 1/6000), Mouse anti-human CD3, BV510 conjugated (BD Biosciences Cat# 563918, Lot 7037566, Clone SP34-2, Dilution 1/20), Mouse anti-human CD4, BV510 conjugated (BD Biosciences Cat# 562970, Lot 7094727, Clone SK3, Dilution 1/80), Mouse anti-human CD8, BV510 conjugated (BioLegend Cat# 301047, Lot B221676, Clone RPA-T8, Dilution 1/80), Mouse anti-human CD14, BV510 conjugated (BioLegend Cat# 301841, Lot B236875, Clone M5E2, Dilution 1/80), Mouse anti-human CD16, BV510 conjugated (BD Biosciences Cat# 563830, Lot 7103547, Clone 3G8, Dilution 1/160), Mouse anti-human CD56, BV510 conjugated (BioLegend Cat# 318339, Lot B205718, Clone HCD56, Dilution 1/40), Mouse anti-human CD19, ECD conjugated (Beckman Coulter Cat# IM2708U, Lot 97, Clone J3-119, Dilution 1/40), Mouse anti-human IgG, BV785 conjugated (BD Biosciences Cat# 564230, Lot 7037913, Clone G18-145, Dilution 1/80), Mouse anti-human IgD, APC-Cy7 conjugated (BioLegend Cat# 348217, Lot B234185, Clone IA6-2, Dilution 1/160), Mouse anti-human IgM, PE-Cy5 conjugated (BD Biosciences Cat# 551079, Lot 7041529, Clone G20-127, Dilution 1/10).

Validation

All antibodies from commercial sources undergo validation using flow cytometry, western blot, chromatin immunoprecipitation, immunofluorescence, immunohistochemistry, and/or biofunctional assays to ensure specificity and to provide clarity for research uses. Specifically, mouse anti-human CD3, BV510 conjugated (Clone SP34-2), mouse anti-human CD16, BV510 conjugated (Clone 3G8), mouse anti-human IgG, BV785 conjugated (Clone G18-145), mouse anti-human IgM, PE-Cy5 conjugated (Clone G20-127) and mouse anti-human CD4, BV510 conjugated (Clone SK3) underwent stringent testing and validation by BD Biosciences to assure that it generates a high-quality conjugate with consistent performance and specific binding activity. The validation process included testing on a combination of primary cells, cell lines and/or transfectant cell models with relevant controls using multiple immunoassays to ensure biological accuracy. BD also performs multiplexing with additional antibodies to interrogate antibody staining in multiple cell populations. Mouse anti-human CD8, BV510 conjugated (Clone RPA-T8), mouse anti-human CD14, BV510 conjugated (Clone M5E2), mouse anti-human CD56, BV510 conjugated (Clone HCD56) and mouse anti-human IgD, APC-Cy7 conjugated (Clone IA6-2) were thoroughly validated by Biolegend. Each antibody was tested using the following criteria: 1.Staining of 1-3 target cell types with either single- or multi-color analysis detailed in the QC specification (including positive and negative controls). The tested cells can be primary cells and/or cell lines known to be positive or negative for the target antigen; 2.Each batch product is validated by QC testing with a series of dilutions to make sure the product is working within expected antibody titer range; 3.Each batch is compared to an internally established "gold standard" to maintain batch-to-batch consistency; 4. When applicable, our products are side-by-side tested with our competitors' products to make sure that BioLegend's products exceed or are at least the same quality; 5.For most tandem dye-conjugated products, color compensation is examined in order to verify tandem integrity.
General statements from Biolegend:
“The specificity and sensitivity of each antibody is thoroughly validated in the New Product Development stage. This is done by staining multiple target cells with either single- or multi-color analysis or by other testing approaches. The QC specifications and testing SOPs and gold standard for each product are then developed”.
In general, each product is tested using the following criteria:
1. Staining of 1-3 target cell types with either single- or multi-color analysis detailed in the QC specification (including positive and negative controls). The tested cells can be primary cells and/or cell lines known to be positive or negative for the target antigen.
2. Each batch product is validated by QC testing with a series of dilutions to make sure the product is working within expected antibody titer range.
3. Each batch is compared to an internally established "gold standard" to maintain batch-to-batch consistency.

Mouse anti-human 4G2,(Biovest/NCCC, Produced from ATCC Hybridoma D1-4G2-4-15 (ATCC® HB-112™) has been described for reactivity and specificity in Henchal et al., 1982. (Henchal, E.A., Gentry, M.K., McCown, J.M. & Brandt, W.E. Dengue virus-specific and Flavivirus group determinants identified with monoclonal antibodies by indirect immunofluorescence. Am. J. Trop. Med. Hyg. 31, 830-836 (1982).

Eukaryotic cell lines

Policy information about cell lines

Cell line source(s)	D1-4G2-4-15 mouse hybridoma (ATCC #HB-112), C6/36 (ATCC #CRL-1660), Vero (ATCC #CCL-81), Expi293F (ThermoFisher Scientific #A14527), DS-2 (ThermoFisher Scientific #R69007), U937-DC-SIGN (ATCC #CRL-3253) and K562 (ATCC #CCL-243) cell lines were utilized in this study.
Authentication	All cell lines were authenticated using short-tandem repeat analysis.
Mycoplasma contamination	Cell lines were not recently tested for mycoplasma contamination.
Commonly misidentified lines (See ICLAC register)	No commonly misidentified cell lines were used in this study.

Animals and other organisms

Policy information about studies involving animals; ARRIVE guidelines recommended for reporting animal research

Laboratory animals	Six to eight week old female Balb/c mice and Ifnar-/- knock-out C57BL/6 female mice were used in this study.
Wild animals	This study did not involve wild animals.
Field-collected samples	This study did not involve samples collected from the field.
Ethics oversight	This study was approved by the Institutional Animal Care and Use Committees (IACUCs) at both the Beth Israel Deacon Medical Center and the U.S. Army Medical Research Institute of Infectious Diseases. Research was conducted in compliance with the Animal Welfare Act and other federal statutes and regulations relating to animals.

Note that full information on the approval of the study protocol must also be provided in the manuscript.

Human research participants

Policy information about studies involving human research participants

Population characteristics	These Phase I ZIKV vaccine clinical trials were described previously in Modjarrad, K., et al. "Preliminary aggregate safety and immunogenicity results from three trials of a purified inactivated Zika virus vaccine candidate: phase 1, randomised, double-blind, placebo-controlled clinical trials", The Lancet 391, 563-571 (2018). Men and women, ages 18 to 49 years, were recruited to participant these vaccination trials. Individuals within the BIDMC and WRAIR studies, NCT02937233, NCT02963909, respectively, were enrolled if they had no history of flavivirus infection or vaccination. In addition, individuals within the WRAIR study had to demonstrate a lack of serologic flavivirus neutralization. Individuals within the Puerto Rican trial were not screened for flavivirus history. In addition, individuals with serologic evidence of human immunodeficiency virus, hepatitis B or C infection were excluded from study participation, along with pregnant or breast-feeding women.
Recruitment	Men and women, ages 18 to 49 years, were recruited to participant these 3 ZPIV vaccination trials. Individuals within the BIDMC and WRAIR studies, NCT02937233, NCT02963909, respectively, were enrolled if they had no history of flavivirus infection or vaccination. In addition, individuals within the WRAIR study had to demonstrate a lack of serologic flavivirus neutralization. Individuals within the Puerto Rican trial were not screened for prior flavivirus infection or vaccination history. For further details see Modjarrad, K., et al. "Preliminary aggregate safety and immunogenicity results from three trials of a purified inactivated Zika virus vaccine candidate: phase 1, randomised, double-blind, placebo-controlled clinical trials", The Lancet 391, 563-571 (2018).
Ethics oversight	These studies were approved by the Beth Israel Deaconess Medical Center (BIDMC), Walter Reed Army Institute of Research (WRAIR), St. Louis University (STL), and Quorum Central (now Advarra Central) Institutional Review Boards and written informed consent was obtained from all participants.

Note that full information on the approval of the study protocol must also be provided in the manuscript.

Clinical data

Policy information about clinical studies

All manuscripts should comply with the ICMJE guidelines for publication of clinical research and a completed CONSORT checklist must be included with all submissions.

Clinical trial registration	NCT 02937233, NCT02963909, and NCT03008122
Study protocol	The full trial protocol is published at Modjarrad, K., et al. "Preliminary aggregate safety and immunogenicity results from three trials of a purified inactivated Zika virus vaccine candidate: phase 1, randomised, double-blind, placebo-controlled clinical trials", The Lancet 391, 563-571 (2018).
Data collection	Participants for the BIDMC and WRAIR trials were enrolled between Nov. 2016 and Jan. 2017. Participants were assessed on days 1, 4, 8, 15, 29, 32, 36, 43, and 157 57 following ZPIV vaccination for ZIKV neutralization. Data were collected and masked to study clinicians. Interim results were published in Modjarrad, K., et al. "Preliminary aggregate safety and immunogenicity results from

three trials of a purified inactivated Zika virus vaccine candidate: phase 1, randomised, double-blind, placebo-controlled clinical trials", The Lancet 391, 563-571 (2018). The Puerto Rican trial study was initiated in 2017 and has not yet reached completion when this manuscript was published in Dec. 2019. Study clinical staff have remained blinded to individual-level results from the interim analysis.

Outcomes

The primary outcomes for each trial was designed to evaluate safety, reactogenicity, and immunogenicity of ZPIV through the primary timepoint of day 57. Participants were assessed on days 1, 4, 8, 15, 29, 32, 36, 43, and 157 57 following ZPIV vaccination for ZIKV neutralization. Interim results were published in Modjarrad, K., et al. "Preliminary aggregate safety and immunogenicity results from three trials of a purified inactivated Zika virus vaccine candidate: phase 1, randomised, double-blind, placebo-controlled clinical trials", The Lancet 391, 563-571 (2018). Overall the vaccine caused only mild or moderate reactogenicity, and by day 57 92% of vaccine recipients seroconverted. Microneutralization geometric mean titers peaked at day 43 and exceeded protective thresholds observed in prior animal models. For the Puerto Rican trial, group assignment still remains masked to study clinicians as this study has not yet reached completion. Study clinical staff have remained blinded to individual-level results from the interim analysis.

Flow Cytometry

Plots

Confirm that:

☒ The axis labels state the marker and fluorochrome used (e.g. CD4-FITC).

☒ The axis scales are clearly visible. Include numbers along axes only for bottom left plot of group (a 'group' is an analysis of identical markers).

☒ All plots are contour plots with outliers or pseudocolor plots.

☒ A numerical value for number of cells or percentage (with statistics) is provided.

Methodology

Sample preparation

Cryopreserved PBMCs were thawed in warm medium containing benzonase, then washed with phosphate-buffered saline (PBS) and stained for viability using Invitrogen Aqua Live/Dead stain. Cells were incubated at 4℃ for 30 minutes with a cocktail of antibodies including: CD3 BV510 (BD Biosciences), CD4 BV510 (BD Biosciences) , CD8 BV510 (BioLegend), CD14 BV510 (BioLegend), CD16 BV510 (BD Biosciences) and CD56 BV510 (BioLegend) as dump channel markers, and CD19 ECD (Beckman Coulter), IgG BV785 (BioLegend), IgD APC-Cy7 (BioLegend) and IgM PE-Cy5 (BD Biosciences). ZIKV E and DENV-2 E were tetramerized and conjugated to BV421 (BioLegend) and BV650 (BioLegend), respectively. To obtain monoclonal antibodies that target quaternary epitopes, primary staining also included live whole ZIKV virions (Paraiba_01) followed by secondary staining using 4G2 (Biovest) conjugated to APC (Thermofisher).

Instrument

FACSAria (Becton Dickinson)

Software

FlowJo, version 9.9.6

Cell population abundance

Less than 5% of the total B cell population was specific for either ZIKV or DENV-2. This information was not used within the analysis, as all whole ZIKV virions, ZIKV E and DENV-2 E triple positive B cells were sorted into lysis buffer, sequenced, cloned and characterized.

Gating strategy

CD19+/IgG+/IgD-/IgM- B cells reactive to ZIKV-E, DENV-E, or whole ZIKV virions were sorted directly into lysis buffer at one cell per well into PCR plates using a FACSAria (Becton Dickinson) and stored at −80°C until subsequent reverse transcription. We focused on sequencing and cloning B cell receptors (BCRs) from DENV-2 E positive B cells with and without cross-reactivity with ZIKV E or whole ZIKV virions. The same sorting strategy was performed from PBMCs obtained from Participant A at week 0, prior to ZPIV vaccination, to determine if MZ4-family members were present prior to vaccination, and at week 2, 2 weeks following first ZPIV vaccination, where high neutralization titers against ZIKV and the 4 DENV serotypes were observed. Sorting at week 8 was performed on a different day compared to PBMCs from Participant A at week 0 and week 2, and the ZIKV-naïve donor. Increased frequencies of antigen-specific and cross-reactive B cells were detected against all antigens (whole ZIKV virions, ZIKV E, and DENV-2 E) between week 0 and week 2 (Extended Data Fig. 1b).

☒ Tick this box to confirm that a figure exemplifying the gating strategy is provided in the Supplementary Information.